

UNIVERSITY OF TARTU  
FACULTY OF SCIENCE AND TECHNOLOGY

Institute of Chemistry



Faysal-Al-Mamun

Development of method for boron determination in basalt fibers

Master's Thesis (30 EAP)

Applied Measurement Science

Supervisors:

Päärn Paiste  
Riho Mõtlep

Tartu 2022

# Table of Contents

<b>1. INTRODUCTION .....</b>	<b>3</b>
<b>2. LITERATURE REVIEW .....</b>	<b>4</b>
2.2. BORON DOPED BASALT FIBER .....	4
2.3. BORON DETERMINATION METHODS .....	6
2.3.1. <i>Fluorometric method</i> .....	6
2.3.2. <i>Ionomeric method</i> .....	6
2.3.3. <i>Atomic Emission/Absorption Spectrometry Methods</i> .....	6
2.3.4. <i>Plasma-Source Methods</i> .....	7
2.3.5. <i>XRF Analysis</i> .....	9
2.3.6. <i>Prompt-gamma ray neutron activation analysis</i> .....	10
2.4. SAMPLE DIGESTION TECHNIQUES .....	10
2.4.1. <i>Alkali Fusion</i> .....	11
2.4.2. <i>Dry Ashing</i> .....	12
2.4.3. <i>Acid Digestion</i> .....	12
<b>3. SAMPLE MATERIALS AND METHODS .....</b>	<b>13</b>
3.1. CHEMICALS AND MATERIALS .....	13
3.2. SAMPLE MATERIALS .....	14
3.3. SAMPLE DIGESTION .....	14
3.3.1. <i>Sample Digestion experiment 1</i> .....	16
3.3.2. <i>Sample Digestion experiment 2</i> .....	16
3.3.3. <i>Sample Digestion experiment 3</i> .....	17
3.3.4. <i>Sample Digestion experiment 4</i> .....	18
3.3.5. <i>Sample Digestion experiment 5</i> .....	19
3.3.6. <i>Preparation of sample materials for XRF analysis</i> .....	19
3.5 ANALYTICAL METHODS .....	20
<b>4. RESULTS AND DISCUSSION .....</b>	<b>21</b>
4.1. EXPERIMENT 1 .....	21
4.2. EXPERIMENT 2 .....	23
4.3 EXPERIMENT 3 .....	25
4.4 EXPERIMENT 4 .....	27
4.4 EXPERIMENT 5 .....	29
4.5. XRF ANALYSIS .....	33
<b>5. CONCLUSION .....</b>	<b>35</b>
<b>6. SUMMARY .....</b>	<b>36</b>
<b>7. ACKNOWLEDGEMENTS .....</b>	<b>36</b>
<b>8. KOKKUVÕTE .....</b>	<b>37</b>
<b>8. REFERENCES .....</b>	<b>38</b>
<b>9. ANNEXES .....</b>	<b>42</b>

## 1. Introduction

Radioactive waste is generated by several activities and industrial processes, including medicine, nuclear research, minerals processing, drinking water purification and of course nuclear power generation. Low-, intermediate- and high-level radioactive waste is hazardous material and requires safe handling, storage and deposition. Conventional radioactive waste management often includes immobilizing waste material in concrete matrix or seal it in concrete containers to shield it from the environment. Heavyweight concrete's high strength and density make it an ideal material for shielding purposes. However, it is costly and hard to work with, so different types of composite materials are preferred. New composite materials must improve the mechanical and shielding properties of the concrete. One option is to use fiber materials to improve concrete mechanical properties. And fibers can be tailored to meet specific needs in the range of application. For instance, natural basalt can be processed to basalt fiber and infused with high percentage of boron oxide. For example, basalt fiber has several benefits as it is natural material and highly resistant to degradation in hostile environment and boron additive is a sink to neutron radiation emitting from high-level radioactive materials. The use of such a fiber in concrete production benefit both mechanical and shielding properties of the concrete. The amount of boron oxide in basalt boron fiber is important for increasing the concrete's radioactive shielding characteristics, and therefore it is necessary to identify the precise amount of boron oxide in basalt boron fiber to evaluate boron efficiency in this application. Non-destructive Prompt gamma-ray nuclear activation analysis is a direct determination of boron oxide in basalt fiber, but this technique is costly and time consuming. For other methods of analysis, the sample must be dissolved. However, use of HF that is needed to dissolve silicates (natural basalt) volatilizes boron (B) and sample dissolution is a significant barrier to precise and reliable B measurements in silicate materials.

In the current study a relatively fast and cost-effective method for determining the amount of boron oxide in basalt boron fiber using MP-AES was developed. Natural basalt samples and basalt boron fiber samples from commercial producers were studied in this research.

The thesis focuses on the determination of optimal digestion parameters for  $\text{Na}_2\text{O}_2$  based alkaline fluxing and the effect of different digestion acids on the recovery of B and other major basalt constituents.

## **2. Literature Review**

### ***2.1. Boron and its uses***

Boron is a metalloid of group 13 (IIIA). Although boron is more electron deficient than carbon and silicon, its chemical characteristics are similar (DeFrancesco & Coca, 2016). Boron is the second most abundant of group 13 elements after aluminum and the 38<sup>th</sup> most abundant element overall. Most soils contain around <10 ppm boron. Boron concentration in rocks ranges from 5 to 100 ppm in basalts and shales and is, on average, around 10 ppm in Earth's crust (Woods, 1994).

Nowadays, boron is a significant component for developing different fields of scientific research. It is an essential component for steel, glass, and different glass films (Woods, 1994). It is widely used in materials developed for nuclear reaction applications and semiconductor wafers as a thermalizing agent and dopant. Also control rods, which are crucial nuclear material, are made of boron carbide.

Boron is also used in metal and alloy production. Borates are used in welding rods and other fluxes due to their strong ability to dissolve metal oxides. Boron content is gradually increasing in amorphous metal alloys used in electrical equipment and magnets; also, borates are used widely in fire retardants. As a form of borates, boron is widely used to preserve wood from decay caused by brown and white rot and discoloration caused by fungus (Sah & Brown, 1997). Boron is also used in medicine, in cancer therapy and drug development (Raaijmakers et al., 1994; Song et al., 2021).

In recent decades boron is frequently utilized in nuclear power as a neutron absorber material, which enables nuclear reactors to be controlled by altering the neutron multiplication factor (Terekhova et al., 2019). Boron carbide is widely used in nuclear absorber rods of the control and protection system (CPS) in nuclear power plants because of its high melting point, manufacturability, and relatively low cost in neutron absorption in a wide range of energies. Boron can also be used as a doping material for different fibers to enhance the shielding characteristics of materials used in nuclear facilities.

### ***2.2. Boron doped basalt fiber***

The development of composite materials reinforced with high-strength fibers such as glass and graphite has generated substantial interest due to their increased strength and rigidity (Brack et al., 2005). Boron doped basalt fiber has a higher strength-to-weight ratio than carbon fibers and is utilized in more demanding applications in the aerospace and defense industries (Brack et al., 2005).

The necessity of radiation shielding is growing in lockstep with increased nuclear technology application areas and due to spent materials flow from decommissioning of old nuclear facilities. Heavy concrete is used as a shielding material for transporting nuclear waste and storing it, but this type of concrete is expensive and complex to prepare (Zorla et al., 2017). Cracking of concrete is also one of the primary causes of nuclear power plant decay. Numerous researchers have explored various cement substitutes, alloys, compounds, mixes, glasses and also fibers in order to enhance concrete performance and durability and also find new cost effective and “greener” alternatives to conventional concrete types utilized in hazardous and radioactive waste storage applications. It is seen that the application of fiber reinforcement in concrete reduces the chance and ratio of crack formation of concrete casks or storage containers (Zorla et al., 2017). Concrete can and should also provide shielding capabilities for the hazardous materials it is intended to contain. One novel application is to use fibers mixed with boron oxide. Fibers enhance concrete strength and boron additive absorbs the neutron flux from nuclear waste. The concentration of boron in the fiber is vital. If the concentration is low, the fiber does not provide sufficient shielding properties to the concrete. But mixing and complete homogenization of basalt boron fiber constituent materials during fiber production can be challenging, which makes correct analytics of the product very important. Basalt boron fiber production includes crushing rock, mixing with boron additive, computer-controlled melting/cooling and fiber drawing process, illustrated in simplified schematic *Figure 1* (Zorla et al., 2017).

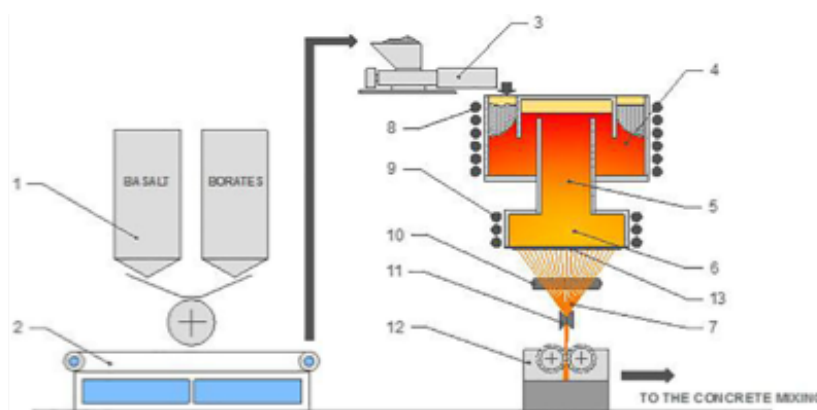


*Figure 1. Scheme of the process for producing the specialty enhanced basalt fibers. 1. Metering & mixing equipment (batch preparation). 2. Conveying equipment. 3. Batch charger. 4. Melting chamber. 5. Conditioning chamber. 6. Fiber forming chamber. 7. Fiber's strand. 8. Induction coil of melting chamber. 9. Induction coil of fiber forming chamber. 10. Sizing applicator. 11. Gathering shoe. 12. Direct chopper. 13. Fiber drawing plate (Zorla et al., 2017)*

### **2.3. Boron determination methods**

Different methods are currently available for determining boron concentrations in various liquid or solid materials. However, the majority of methodologies require dissolution of sample into solution and solute analysis can be sensitive to other matrix components or the pH of the sample.

#### **2.3.1. Fluorometric method**

B is measured using the fluorometric approach, based on the formation of fluorescent complexes of B and measurement of the fluorescence induction at a specific wavelength. The main difference between the various fluorometric methods lies mainly in the reagents used to form fluorescent compounds (Motomizu et al., 1991). This approach, however, is pH and temperature-dependent and suffers from inferences from different chemical species. So, as a result, fluorometric methods are not frequently used to determine boron concentration.

#### **2.3.2. Ionometric method**

In potentiometric determination, B is typically isolated from the sample matrix, treated with HF, and the resulting tetrafluoroborate ion ( $\text{BF}_4^-$ ) is measured potentiometrically using an appropriate  $\text{BF}_4^-$  selective electrode (Sah & Brown, 1997). However, the sample matrix has a considerable impact on these methods, which may alter the potential value. To obtain reliable findings, either the matrix must be removed, or the calibration matrix must be matched to the sample matrix (Yilmaz et al., 2007). A polarographic technique based on the adsorptive properties of the B complex with beryllium (III) (4-((4-diethylamino-hydroxyphenyl)-azo)-5-hydroxy-2,7-naphthalenedisulfonic acid) at the dropping mercury electrode in a solution of potassium hydrogen phthalate (pH 3.7–4.6) was reported for the determination of trace amounts of B ( $1 \times 10^{-9}$  g/mL detection limit) in foods (Lu et al., 1994). The levels of B determined with this method were found to be comparable to those obtained with the ICP-OES method. Although this method is not widely adopted, it remains an option for the determination of boron in borophosphosilicate glass, rocks, ores, and environmental materials (Wood & Nicholson, 1994).

#### **2.3.3. Atomic Emission/Absorption Spectrometry Methods**

Atomic emission spectrometry (AES) and atomic absorption spectrometry (AAS) both need the introduction of samples into a flame (often acetylene–air or acetylene– $\text{N}_2\text{O}$ –air) in order to atomize the elements, present in the sample. The AAS method is based on the idea that unbound atoms of a particular element (e.g., B) absorb photons with distinct energy values (a

characteristic wavelength) generated by a hollow cathode lamp containing that element (e.g., B) (Sah & Brown, 1997). AES methods are used to determine the emission of atomized and excited species as they fall to the ground state. For adequate reading of boron in AES/AAS determination, it is frequently necessary to separate and preconcentrate B from the sample matrix (Raja et al., 2020). It has been shown that analysis of B separated as volatile methyl borate from the sample matrix, by atomic emission measurements of the  $\text{BO}_2^-$  radical at 548 nm (Jeyakumar et al., 2008) or absorbance measurement at 149.7 nm (Sarica & Ertas, 2001) enhanced the detection limit and sensitivity. This method however has low sensitivity, significant memory effects from prior samples and numerous interferences (Burguera et al., 2001).

The Electro Thermal Atomization Atomic Absorption Spectrometry (ET-AAS) method can be used to analyze solid or liquid samples without simple digestion by utilizing high-temperature atomization (Krejčová & Černohorský, 2003; Resano et al., 2007). Without chemical modifiers, the ET-AAS method has a low detection limit and sensitivity due to inefficient thermal dissociation of B-containing species (oxides and carbides) generated by dissociative desorption of  $\text{B}_2\text{O}_3$  and severe memory effects caused by B atoms undergoing a series of condensation–vaporization steps, resulting in an endless plain in the tail of AAS signals (Volynskii, 2003). Chemical modifiers and treatment of the pyrolytic graphite tube are frequently required to obtain acceptable ET-AAS findings. Coating the graphite tube with tungsten carbide or lanthanum carbide enhanced the pyrolysis temperature of B from 850°C to >2200°C, and adding a Ca–Mg modifier to the B solutions boosted the pyrolysis temperature to 1200°C (pez-García et al., 2009). Increased pyrolysis temperature is expected to improve the thermal dissociation efficiency of B-containing compounds. A chemical modifier including nickel and zirconium salts and treatment of the graphite tube with zirconium solution mitigated the effect of iron on the determination of B in iron and nickel-based alloys using ET-AAS (de Lima et al., 2003). Diammonium hydrogen phosphate (DHP) and NaOH were used as chemical modifiers to decrease matrix interferences and to keep the determined same on the tungsten boat furnace vaporizer's surface during the ET vaporization process. (Tu et al., 2010). The ideal conditions for determining ET-AAS in cell suspension B were a 4-second hold duration at 2500°C for atomization and a 249.7 nm detection wavelength (Carrero et al., 2005).

#### **2.3.4. Plasma-Source Methods**

The introduction of plasmas as ionization sources and the development of plasma-source analytical instruments (plasma-source OES and MS) enabled the determination of B with

greater sensitivity and a lower detection limit than was previously possible using spectrophotometry flame AES/AAS and time-consuming nuclear methods (Sah & Brown, 1997). There are various forms of plasmas: direct current plasmas (DCP), inductively coupled plasmas (ICP), microwave-induced plasmas (MIP), and glow discharge plasmas (GDP) (Aramendía et al., 2015; Rietig & Acker, 2017). Plasmas can be formed using a variety of gases or mixes of gases; however, most commercial plasma-generating equipment uses an argon ICP (i.e., an ICP generated from argon) for ionization (Richardson, 2001). There are two types of plasma source instruments: those that use plasma-source optical emission spectrometry (OES), such as ICP-OES and DCP-OES, and those that use plasma-source mass spectrometry (MS), such as ICP-MS, DCP-MS, and microwave-induced plasma (MIP)-MS. Although by default, samples are converted to liquid and introduced into the instruments' plasma as aerosol, several alternate modes of sample introduction (e.g., slurry, powder, gases, laser ablation, and electrothermal vaporization (ETV)) can be used for specific purposes, primarily to avoid sample preparation and to minimize interferences (Ammann, 2007). In general, the presence of HF in the digest impairs B determination and has a strong influence on the sample introduction and interface areas of the plasma-based instruments (Sah & Brown, 1997). Before determining with a plasma source, HF should be eliminated from the sample by evaporation to dryness (Sah & Brown, 1997).

Elements like B, P, and Mo are difficult to analyze trace level with AAS and ICP-OES because of high LODs and LOQs, but with the use of microwave plasma atomic emission spectrometry (MP-AES) these problems can be overcome (Sreenivasulu et al., 2017). MP-AES benefits in this application are that it has low detection limits, a wide linear range, and the ability to detect multiple elements at the same time. MP-AES is a multi-element technique that, in comparison to FAAS, provides higher detection limits over a more comprehensive analytical working range. Unlike prior microwave-induced plasma (MIP) sources, this technology employs a unique magnetically stimulated emission source connected to an emission spectrometer. The resulting plasma shape is comparable to that produced by a standard ICP nebulizer and a spray chamber, allowing for simple entrainment of the wet sample aerosol into the plasma core. (Sreenivasulu et al., 2017). In both MP-AES and ICP-OES, identical wavelengths (249.677 nm for B) were used to measure emission signals. The concentration of the analyte was determined using a direct comparison of the various signals in the linear range rather than the standard method, which depends on reasonable extrapolations (Vudagandla et al., 2017). During analysis, it was also seen that if the sample contains more iron, then the boron signal can get



interfered by the Fe signal. Si interferences can also be problematic when low concentrations of boron need to be analyzed.

The ICP-MS has an advantage over other methods because of its lower detection limit and higher sensitivity. The most precise boron determination is done by using the isotope dilution method for quantitative analysis (Dai et al., 2014). The external calibration method with an internal standard is also a widely used method for ICP-MS. The external calibration method works well for liquid samples with simple matrices, but for complex matrices, the isotope dilution method is used to improve precision. In ICP-MS, sequential use of different rinse solutions of 2% HNO<sub>3</sub>, ultrapure water, and 2% ammonium solution has been used to remove the memory effects of boron during the analysis (Dai et al., 2014). The tendency of boron in the sample solution to volatilize as boric acid on the inside surface of the ICP-MS spray chamber is the main reason for this boron memory effect but by using ammonia solution it is possible to neutralize the volatile boric acid to a nonvolatile compound (NH<sub>4</sub>H<sub>2</sub>BO<sub>3</sub>) on the surface (Dai et al., 2014).

In conclusion it is seen that among plasma methods ICP-MS method is good for determination of boron in lower level of detection but it is also seen that with MP-AES it is also possible to determine the boron concentration which result is closer with ICP-MS but both methods need some sample treatment because of interferences. By doing necessary sample treatment it is possible to remove some interferences and the determination will be more accurate.

### **2.3.5. XRF Analysis**

Presently, X-Ray fluorescence is the most popular and effective technology for determining qualitatively and quantitatively a vast majority of elements contained in ceramic materials, including raw materials and frits or glasses with complicated and changeable compositions (Sanchez-Ramos et al., 2000). Normally it is difficult to analyze ultralight elements like boron with XRF because of standard method of sample preparations as glass disc but due to temperature effect there can be some bubble present in the glass disc. Some researchers have been able to determine the boron in different silicate samples with XRF. van Spang & Bekkers (1998) used XRF technique to determine boron in boron-phosphorus-silicon glass. The samples were in the form of pellets.

XRF may be used to measure  $B_2O_3$  in glass discs using boron-rich melts with known boron contents, allowing this method to be used to samples with low boron concentration since the signal is amplified by the boron added to the melt (Sanchez-Ramos et al., 2000). In addition of using  $Li_2B_4O_7$  dilutes and homogenizes the sample, reducing the matrix effect. It enables calibrations with large boron percentages (Sanchez-Ramos et al., 2000).

Although XRF technique can be used to determine boron concentration in different glass or ceramic samples, extensive sample preparation is needed to produce glassy materials for analysis.

### **2.3.6. Prompt-gamma ray neutron activation analysis**

Prompt-gamma ray neutron activation analysis (PGNAA) is a non-destructive technique for determining B in solid samples (Montesano et al., 1991). All elements can theoretically be analyzed with PGNAA, however it is most commonly used for elements with favorable nuclear properties, such as high (neutron, gamma) cross sections and suitable isotopic abundance. One of the big advantages of this technique is that contamination of samples can be avoided (Acharya, 2009).

The boron concentrations in a variety of samples, including reference materials, have been measured using this technique, ranging from traces to large contents (Chen-Mayer et al., 2000). Some experiment like for food items, accurate quantification ranged from 1.0 to 2.5 mg/kg B, whereas detection limits ranged from 0.3 to 0.8 mg/kg B depending on the irradiation time (Yonezawa & Wood, 1995). When boron is present in larger concentrations (mass > 1 mg), neutron self-shielding leads to errors in the boron determination, as do higher background counts under 478 ke V and gamma-ray interferences (Copley & Stone, 1989).

The main drawback of this technique is that it needs a nuclear reactor for the source of thermal neutrons. In conclusion though this method has some drawbacks, it is still one of the most extensively used methods for the determination of boron in medical science and boron neutron capture therapy (Sah & Brown, 1997).

### **2.4. Sample Digestion techniques**

For analysis of boron using plasma or flame based spectroscopic techniques the sample must first be digested and brought into liquid medium. Boron-containing samples can be digested using a variety of methods. However, analyte losses can cause incorrect findings if sample

preparation isn't done correctly. Most notable loss of boron can occur when HF is used for sample preparation as boron can be volatilized as  $\text{BF}_3$ . Significant amounts of B may be lost during the decomposition and the evaporation processes, owing to the high volatility of  $\text{BF}_3$ , if proper precautions are not taken. The volatilization loss of B during the evaporation process occurs more readily from acidic solutions than from neutral or alkaline solutions (Sah & Brown, 1997). Alkali fusion process for digestion of B samples is found to be most effective and precise when compared to other sample digestion systems. However, different sample matrixes necessitate the use of different methods of digestion. The methods for dissolving samples for B determination are outlined in the following section.

#### **2.4.1. Alkali Fusion**

The alkali fusion method is usually used for solid materials such as soil and geological samples. In this fusion technique, the sample is generally fused with alkali (mainly  $\text{K}_2\text{CO}_3$  or  $\text{Na}_2\text{CO}_3$ ) and then dissolved in acidic medium for analysis. Recently, this technique was used with  $\text{Na}_2\text{O}_2$  as the alkali agent to determine B and its isotopic composition in silicate geological reference materials by Cai et al., (2021), based on sintering methods used by (Kleinhanns et al., 2002; Meisel et al., 2002). Powdered sample aliquots of 100 mg were mixed with ground  $\text{Na}_2\text{O}_2$  beads in a glassy carbon crucible at flux to sample ratios of 5 or greater, placed in a muffled furnace at  $490^\circ\text{C}$ , and heated for 30 minutes. After the sample cooled down to room temperature water was dropwise added to the sintered cake where the reaction started vigorously. After addition of 3 ml of water, the alkaline suspension was transferred into centrifuge tubes and the remaining residue was dissolved with concentrated HCl and added to the tube (Cai et al., 2021). The samples were then subjected to column chemistry procedure using Amberlite 473 resin to selectively separate B from other matrix components using 2% nitric acid. Meisel et al., (2002) showed that powdering the granular  $\text{Na}_2\text{O}_2$  improves the sintering efficiency. Apart from proper weighing and aliquoting of the solutions, the following must be ensured to obtain reliable findings for concentration measurements when using isotope dilution (ID) methodology: (1) total dissolution of the sample; (2) complete equilibration of the sample aliquot with the spike. When performed adequately, i.e., with sufficient reagent and thorough mixing of the sample and powdered reagent, the sodium peroxide sintering process provides complete sample dissolution and boron recovery (Cai et al., 2021).

Tonarini et al., (1997) used  $\text{K}_2\text{CO}_3$  based fusion for boron isotopic analyzing in silicate rock sample. In that method pure  $\text{K}_2\text{CO}_3$  was used as the flux due to its high solubility, which enables quick water leaching of the resulting fusion cakes. Finely powdered samples (0.2-1.0 g) were

mixed with pure  $K_2CO_3$  with flux to rock ratio 5:1 in Pt crucibles and kept at  $1000^\circ C$  in the muffle furnace (Tonarini et al., 1997). When the fusion cakes were completely cooled, they were dissolved in 5-6 mL ultrapure  $H_2O$  at room temperature and then placed into polypropylene tubes (Tonarini et al., 1997).

In conclusion, it can be seen that the approach has the advantage of being able to handle a large volume of material while also allowing for the processing of rocks with low boron concentrations. Additionally, it was an alternative method of boron extraction from silicate materials to replace the HF-based methods, such as developed by Nakamura et al., (1992).

#### **2.4.2. Dry Ashing**

Usually, plant dried tissue or different types of solid plant samples are prepared using this technique as the aim is to quantify the boron incorporated in the organic phase. In this approach, the dried sample is ashed in a muffle furnace using platinum or quartz crucible, and after that, the resulting ash is dissolved using dilute acid like  $HNO_3$  (Sah & Brown, 1997). During the ashing in the muffle furnace, there is a possibility of losing some analyte from the sample when the temperature is more than  $80^\circ C$ . Therefore, it is important to control the temperature during the ashing to overcome the loss of analyte. In a previous study (Al-Warthan et al., 1993), a combination of ashing with alkali treatment was investigated. In the study, dates seed were treated with saturated  $Ca(OH)_2$ , dried at  $105^\circ C$  and dry ashed in a muffle furnace and dissolved in water for determination of boron (Al-Warthan et al., 1993).

#### **2.4.3. Acid Digestion**

The decomposition of rock samples and the subsequent chemical separation of the elements are usually performed using acids such as HF, HCl,  $HNO_3$ ,  $HClO_4$  or  $H_2SO_4$ . However, in these acid solutions (especially in HF and HCl), boron is easily volatilized as gaseous species such as  $BF_3$  or  $BCl$ , with the consequence that a large boron isotopic fractionation result (Nakamura et al., 1990).

While drying silica digests to near-dryness, Hu (1991) used Mannitol to control B volatilization during the evaporation of the HF/ $HNO_3$  from the digests (0.5 mL volume). On the other hand, Li-Qiang & Zhu (1986) used orthophosphoric acid ( $H_3PO_4$ ) instead of mannitol and achieved 100% recovery of B following the evaporation of the digests to dryness at  $70^\circ C$ .

In this sample digestion method with orthophosphoric acid ( $H_3PO_4$ ), it is observed that some volatilization losses of B occurred, but losses of B are less than in the case of dry ashing method and the yields are better (Banuelos et al., 1992; Hu, 1991; Li-Qiang & Zhu, 1986)

Biological samples can also be digested with  $\text{HNO}_3$  and  $\text{H}_2\text{SO}_4$  in borosilicate digestion tubes (Banuelos et al., 1992). In this technique, samples were first placed into a borosilicate digestion tube and then a specific amount of  $\text{HNO}_3$  (according to sample size) was added; later on,  $\text{H}_2\text{SO}_4$  was added to the sample and kept for 12 to 24 hours in a heating block at  $180^\circ\text{C}$  for oxidation (Banuelos et al., 1992). Samples were removed from the heating block and allowed to cool to room temperature when the  $\text{HNO}_3$  fumes evaporated (Banuelos et al., 1992).

### **3. Sample Materials and Methods**

#### ***3.1. Chemicals and materials***

Trace metal grade  $\text{HNO}_3$  and  $\text{HCl}$  were used in sample treatment. Ultra-pure deionized water ( $18.2\Omega$ ) was produced using a Milli-Q water purification system. Deionized water was mixed with reagent grade  $\text{HNO}_3$  to generate a 2% (v/v) solution of  $\text{HNO}_3$  that was used for sample dissolution and dilution. Liquid sample dilution and storage were done in 12 ml PP (polypropylene) tubes rinsed three times with Milli-Q water. Zirconium crucibles were used to mix the sample with the  $\text{Na}_2\text{O}_2$  and perform fusion using Katanax X300 electric furnace fusion fluxer. The  $\text{Na}_2\text{O}_2$  used for the research is laboratory grade Sigma Aldrich  $\text{Na}_2\text{O}_2$ , ACS Reagent beads with 95% purity. Agate mortar and pestle were used to grind the  $\text{Na}_2\text{O}_2$  to powder form. Laboratory grade  $\text{H}_3\text{BO}_4$  was used for boron additions. After sintering, zirconium crucibles were transferred into 100ml PFA beakers. Small magnetic bars (2 mm in diameter and 7 mm in length) were used to mix the sinter solution after addition of liquids. Boron fibers (commercial sample) were milled with Retsch PM 100 planetary ball mill with 25 agate balls (diameter of the balls is 10 mm) in 80 ml agate lined milling bowl with addition of Milli-Q water or ethanol. For preparation of calibration standards for MP-AES measurements, 1g/L single element standards were used. To matrix match the calibration standards to the sample solutions the standards were prepared using 2%  $\text{HNO}_3$  solution containing the same amount of Na as the sample solutions that were subjected to measurement. The Na in 2%  $\text{HNO}_3$  solution was prepared by dissolving laboratory grade  $\text{NaHCO}_3$  that was dried overnight at  $105^\circ\text{C}$  to a final concentration of 250 mg/L Na. All sample dilutions were prepared to match the Na content in sample solutions to Na in the calibration standards, assuming that all Na originated from  $\text{Na}_2\text{O}_2$  as the additional Na from the sample material accounts to a maximum of around 1% of the total Na content in the final solutions.

### **3.2. Sample materials**

Two different type of sample materials were used. First, laboratory made natural basalt and boron mixtures were made for the reference, and second, basalt-boron fibers with pre-described  $B_2O_3$  concentrations were obtained from the Institute of Physics, UT. Those fibers and had been used in previous studies. The basalt fiber samples were named after their commercial producers as Chernvitsi (6% and 12% of  $B_2O_3$  in fiber) and Bavoma (6% and 12% of  $B_2O_3$  in fiber).

The reference basalt-boron material was prepared with natural basalt from Iceland (from the University of Tartu geology laboratory). Basalt was crushed and milled using Retsch PM 100 planetary ball mill using an 80ml grinding bowl with tungsten carbide inset and 20 mm tungsten carbide balls. Aliquots of this homogenized powder were doped with various concentrations of boric acid ( $H_3BO_3$ ) to produce mixtures with different mass fractions of  $H_3BO_3$  (1%, 4%, 6%, 10%, 12%). In doping process, appropriate amounts of natural basalt and boric acid were weighed into an 80 ml grinding bowl with tungsten carbide inset and milled using 10 mm tungsten carbide balls to ensure homogenous distribution of the boric acid.

### **3.3. Sample Digestion**

To validate the efficiency of the digestion methods and to determine the optimal digestion conditions several experiments with boron doped natural basalt and commercial basalt fibers were undertaken. All solutions were analyzed on the same day as the digestions were prepared, to reduce the risk of analyte loss via adsorption or precipitation (mainly through silica). The following paragraphs outline the experimental details. All sample- $Na_2O_2$  fusions were performed using the following sample preparation guide and fusion regime on Katanax X300 electric furnace fusion fluxer. An agate mortar was used to grind up sodium peroxide, originally sold in granular bead form. Dry sample material (dried overnight at  $105^\circ C$ ) was weighed into zirconium crucibles and a pre-described amount of ground  $Na_2O_2$  was added. The sample and sodium peroxide were thoroughly mixed with a plastic spoon, and the zirconium crucibles were rotted by hand to ensure thorough mixing. The crucibles were then placed into the fluxer and the fusions were performed according to steps in [Table 1](#). In all sample digestions experiments, the fusion method was kept constant and unchanged. The schematic outline of the sample preparation procedure is described in [Table 2](#).

*Table 1. Fluxing method for sample - Na<sub>2</sub>O<sub>2</sub> mixture on Katanax X300*

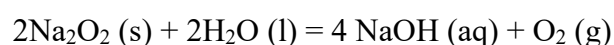
Step	Temperature °C	Time (minutes)	Ramp of Temperature °C	Rocking angle (°)	Speed Percentage (%)
1	550°C	0:30	Fast	0°	0%
2	650°C	n.a.	40°C/min	0°	0%
3	750°C	1:00	Fast	0°	0%
4	750°C	n.a.	Fast	0°	0%
5	750°C	2:00	Fast	25°	100%
6	750°C	1:00	Fast	30°	5%
Pouring	<b>No Pouring</b>				

*Table 2. Preparation steps of boron fiber sample for MP-AES*

Step	Sample Condition	Volume(ml) of liquid
Cut the fiber	The solid form of fiber	--
Milling	The fiber was milled with 25-piece 10 mm agate balls	3 ml of Milli-Q water/ethanol
Drying	Sample dried in an oven overnight at 105°C	--
Sintering	The dried samples were transferred to a zirconium crucible and sintered with Na <sub>2</sub> O <sub>2</sub> in an electric furnace at 750°C.	--
Transfer for dissolving	The zirconium crucible was transferred into a Teflon beaker	--
Dissolving Step 1	Added Milli-Q water dropwise to the flux cake	3 ml of Milli-Q water
Dissolving Step 2	After completing the reaction with water, concentrated acid was dropwise added to the sample solution	3/6 ml Concentrated HCl/HNO <sub>3</sub>
Final Dissolving step	2% HNO <sub>3</sub> was added to complete the final solution	100 ml of HNO <sub>3</sub> (2%)

### 3.3.1. Sample Digestion experiment 1

For the first experiments, the natural basalt was milled, and then the basalt powder was mixed with different percentages of boric acid ( $\text{H}_3\text{BO}_4$ ). The weight % of boric acid used were 1%, 6%, and 12% of the total sample mass. Two sets of samples were prepared. One was 5:1 (flux to sample), and another was 10:1 (flux to sample ratio). The sample size and  $\text{Na}_2\text{O}_2$  were constant at 0.1 g and 0.4 g for the 5:1 ratio and 0.1 g and 0.9 g for 10:1. Samples were weighed straight into dry Zirconium crucibles. After weighing the sample, the  $\text{Na}_2\text{O}_2$  was also weighed together with the sample in the zirconium crucibles. The sample and sodium peroxide were thoroughly mixed with a plastic spoon. The samples were then placed into the furnace and fluxed according to the method described in [Table 1](#). After collecting the zirconium crucible from the furnace, the samples were cooled down to room temperature, and the crucibles were placed in Teflon beakers. A plastic watch glass with a hole in the center was placed on top of the Teflon beaker and 3 ml of Milli-Q water was added to the sintered material dropwise with a pipet until vigorous fizzling reaction had subsided. The fizzing occurs because of the reaction between water and unreacted  $\text{Na}_2\text{O}_2$  that produces oxygen.



The Teflon beakers were also turned by hand so that the sinter attached to the wall of the zirconium crucibles would be better dissolved. 6 ml of concentrated  $\text{HNO}_3$  was added to the 10:1 ratio samples (0.9 g of  $\text{Na}_2\text{O}_2$  and 0.1 g of basalt mix with boric acid sample), and 3 ml of concentrated  $\text{HNO}_3$  to the 5:1 ratio samples (0.4 g of  $\text{Na}_2\text{O}_2$  and 0.1 g of basalt mix with boric acid sample) dropwise with an automatic pipet through the watch glass to dissolve the remaining sample. After the addition of the concentrated nitric acid, 50  $\mu\text{l}$  of solution was removed and diluted in 2%  $\text{HNO}_3$ . Next, 100 ml of 2%  $\text{HNO}_3$  was added while washing liquid droplets from the watch glass to the Teflon beaker. Magnetic stirrers were added to the beakers and were heated at 40°C whilst rotating the stirring magnets at 250 rpm on a magnetic hotplate for 5 min. The samples were collected into 12 ml PP tubes and diluted using 2%  $\text{HNO}_3$  to achieve Na concentrations of 250 mg/L.

### 3.3.2. Sample Digestion experiment 2

After seeing the result of experiment one, the second experiment was conducted using different dissolving acids. In this experiment, two sets of samples were prepared for dissolving with



concentrated HNO<sub>3</sub> and HCl. Basalt (without boric acid) and 6% and 12% of boric acid basalt mixes were used as samples. Again, two sets of samples were prepared, but the sample size and Na<sub>2</sub>O<sub>2</sub> were kept constant at 0.1 g and 0.9 g, as a ratio of 10:1. The samples were fused according to the method in *Table 1*.

After collecting the samples from the furnace, they were cooled down to room temperature and were placed in the Teflon beakers with magnet bars. 3 ml of Milli-Q water was added dropwise to every crucible and covered with watch glass until the reaction ended. In the meantime, the crucibles were tilted so that the sample material attached to the crucible's inner wall also dissolved.

One set of samples was then further dissolved with concentrated HNO<sub>3</sub>. After adding 3 ml of Milli-Q water, 3 ml of concentrated HNO<sub>3</sub> were added to the samples dropwise so that the remaining sample dissolved. 100 ml of 2% HNO<sub>3</sub> was added while washing liquid droplets from the watch glass to the Teflon beaker. Magnetic stirrers were added to the beakers and were heated at 40°C whilst rotating the stirring magnets at 250 rpm on a magnetic hotplate for 5 min.

The other set of samples was dissolved with concentrated HCl. After adding 3 ml of Milli-Q water, 3 ml of concentrated HCl were added to the samples dropwise for the remaining sample to be dissolved. 100 ml of 2% HNO<sub>3</sub> was added while washing liquid droplets from the watch glass to the Teflon beaker. Magnetic stirrers were added to the beakers and were heated at 40°C whilst rotating the stirring magnets at 250 rpm on a magnetic hotplate for 5 min. After dissolution, all samples were collected into 12 ml PP tubes and diluted using 2% HNO<sub>3</sub> to achieve Na concentrations of 250 mg/L.

### **3.3.3. Sample Digestion experiment 3**

In this experiment, two sets of the sample were prepared for dissolving with HNO<sub>3</sub> and HCl. Basalt (without boric acid) and 6% and 12% of basalt mixed with boric acid were used as samples. Again, two sets of samples were prepared, but this time the sample size and Na<sub>2</sub>O<sub>2</sub> were kept constant at 0.2 g and 1.8 g to validate if the sample amount at 10:1 ratio has an effect on the dissolution efficiency.

The samples digested with concentrated HNO<sub>3</sub> were run two times in the furnace as after the first run, the flux cakes visually differed from the flux cakes of previous experiments. After heating two times in the furnace, the sample was cooled to room temperature and transferred

into Teflon beakers. Teflon beakers were covered with watch glass. 3 ml ultra-pure water was added to the zirconium crucibles drop by drop until the reaction was complete and no further fizzing was noticed from the crucibles. 6 ml of concentrated HNO<sub>3</sub> was added to the beakers and after that, 100 ml of 2% HNO<sub>3</sub> was added while washing liquid droplets from the watch glass to the Teflon beaker. Magnetic stirrers were added to the beakers and were heated at 40°C whilst rotating the stirring magnets at 250 rpm on a magnetic hotplate for 5 min.

The same process was used for another group of samples that were subjected to dissolution with HCl. The samples for HCl digestion were heated once in the furnace, and the remaining procedures were identical to those for the concentrated HNO<sub>3</sub>-digested samples.

After dissolution, all samples were collected into 12 ml PP tubes and diluted using 2% HNO<sub>3</sub> to achieve Na concentrations of 250 mg/L.

#### **3.3.4. Sample Digestion experiment 4**

Three boron doped basalt fiber samples from two different producers were used. Two samples were from producer Chernvitsi which were labeled to contain 6% and 12% of B<sub>2</sub>O<sub>3</sub>, according to the supplier. Third sample supplied by producer Bavoma was labeled to contain 12% of B<sub>2</sub>O<sub>3</sub>, according to the supplier.

First, fibers were cut into small pieces so that they can be better milled in the planetary ball mill. For milling those fibers, 25 agate balls with 10 mm diameter were used in a 80 ml agate lined grinding jar. Milling was performed in liquid medium i.e. using wet milling to facilitate the milling process. The fibers (0.5-1 g) were weighed in the 80 ml grinding jar and 3 ml of Milli-Q water (for Chernvitsi) or 3 ml of ethanol (for Bavoma) was added to the fiber samples. Ethanol was used on Bavoma sample due to time constraints to speed up drying process after milling. For milling, ball to sample weight ratio above 20:1 was employed to ensure efficient milling conditions. The milling was performed at 500 rpm in 3 milling cycles each lasting 2 min with 30 s of cooling time in between individual cycles. After milling, the wet slurry was collected in a ceramic evaporating dish by washing the balls and jar with sufficient amounts of the same liquid that was used in milling and Chernvitsi samples were dried overnight in an oven at 105°C and Bavoma sample was dried at 70°C until it was dried out.

After collecting the powder form of the sample from the oven, they were allowed to cool down to room temperature. Two different sample weights were tested whilst keeping the flux to

sample ratio of 10:1. Weight of the sample and Na<sub>2</sub>O<sub>2</sub> used were 0.2 g sample to 1.80 g Na<sub>2</sub>O<sub>2</sub> and 0.1 g of sample to 0.9 g of Na<sub>2</sub>O<sub>2</sub>. After heating in the furnace following the procedure outlined in Table 1, the samples were cooled to room temperature and transferred into Teflon beakers. 3 ml of ultra-pure water was added to the zirconium crucibles drop by drop until the reaction was complete and no further fizzing was noticed from the crucibles. 3 or 6 ml of concentrated HCl was dropwise added to the samples. 3 ml was used for fluxes with 0.1 g basalt sample and 6 ml for fluxes with 0.2 g basalt sample. 100 ml of 2% HNO<sub>3</sub> was added while washing liquid droplets from the watch glass to the Teflon beaker. Magnetic stirrers were added to the beakers and were heated at 40°C whilst rotating the stirring magnets at 250 rpm on a magnetic hotplate for 5 min. After dissolution, all samples were collected into 12 ml PP tubes and diluted using 2% HNO<sub>3</sub> to achieve Na concentrations of 250 mg/L.

### **3.3.5. Sample Digestion experiment 5**

Two powdered samples prepared from basalt fibers supplied by producer Bavoma with expected B<sub>2</sub>O<sub>3</sub> concentrations of 6% and 12% were used in the final experiment. Two different sample weights were tested whilst keeping the flux to sample ratio of 10:1. Sample and Na<sub>2</sub>O<sub>2</sub> masses used were 0.2 g sample to 1.80 g Na<sub>2</sub>O<sub>2</sub> and 0.1 g of sample to 0.9 g of Na<sub>2</sub>O<sub>2</sub>. After heating in the furnace following the procedure outlined in Table 1, the samples were cooled to room temperature and transferred into Teflon beakers. 3 ml ultra-pure water was added to the zirconium crucibles drop by drop until the reaction was complete and no further fizzing was noticed from the crucibles. 3 or 6 ml of concentrated HCl was dropwise added to the samples. 3 ml was used for fluxes with 0.1 g basalt sample and 6 ml for fluxes with 0.2 g of basalt sample. 100 ml of 2% HNO<sub>3</sub> was added while washing liquid droplets from the watch glass to the Teflon beaker. Magnetic stirrers were added to the beakers and were heated at 40°C whilst rotating the stirring magnets at 250 rpm on a magnetic hotplate for 5 min. After dissolution, all samples were collected into 12 ml PP tubes and diluted using 2% HNO<sub>3</sub> to achieve Na concentrations of 250 mg/L.

### **3.3.6. Preparation of sample materials for XRF analysis**

Two sets of boron doped natural basalt samples alongside with 3 commercial boron doped basalt fibers (Bavoma 6%, Chernvitsi 6% and 12% B<sub>2</sub>O<sub>3</sub>) were subjected to XRF measurements to characterize the B signal from different doping techniques. Due to limited sample quantity Bavoma 12% sample was not characterized. Doping of the natural basalt was done using boric

acid or 50/50 LiTB ( $\text{Li}_2\text{B}_4\text{O}_7$ )/LiMB ( $\text{LiBO}_2$ ). Samples containing 4%, 6%, 10% and 12% of boric acid ( $\text{H}_3\text{BO}_3$ ) by weight were prepared using the description outlined in chapter 3.2 In the case of LiTB/LiMB the natural basalt sample were weighed into an agate mortar and appropriate amount of LiTB/LiMB was added and mixed by milling using an agate pestle. Boric acid-based samples were prepared as mixtures containing 4%, 6%, 10% and 12%  $\text{H}_3\text{BO}_3$  by weight and LiTB/LiMB based samples were prepared as mixtures containing 4%, 8% and 12%  $\text{B}_2\text{O}_3$  by weight. Around 5g of powder samples were then pressed into a disc using a hydraulic press, by applying 40 tons of pressure. Pressed powder discs of dry milled Chernvitsi and Bavoma samples were obtained from previous projects as the sample amount available for this study was insufficient.

### ***3.5 Analytical methods***

The chemical composition of the natural basalt was determined using X-ray fluorescence analysis on Rigaku Primus II spectrometer. Prior to the analysis the sample was fused into a glass disk using 50/50 LiTB ( $\text{Li}_2\text{B}_4\text{O}_7$ )/LiMB( $\text{LiBO}_2$ ) at sample to flux ratio of 1:10 with Katanax X300 electric furnace fusion fluxer. The same XRF instrument was also used to characterize the boron  $\text{K}\alpha$  spectral region of commercial fiber samples and  $\text{H}_3\text{BO}_3$  or LiTB/LiMB doped pressed powder samples. Analysis of all dissolved samples was performed on Agilent 4210 MP-AES (Microwave Plasma Atomic-Emission Spectroscopy) that utilizes nitrogen-based plasma. Instrumental parameters for MP-AES measurements are outlined in [Table 3](#).

Samples from experiment 5 were also analyzed in duplicate using Agilent 8800 ICP-MS in the Department of Geology at the University of Tartu. The calibration standards for MP-AES measurements were prepared by mixing 1 g/L single element stock solution that were diluted to appropriate concentrations using 2%  $\text{HNO}_3$  containing 250 mg/L Na. The calibration solutions were prepared in the range of 0.1 mg/l to 5 mg/l for B, 0.4 mg/l to 20 mg/l for Al, Fe, Ca and 1 mg/l to 50 mg/l for Si. A secondary calibration standard was measured every 4-6 samples and a second order polynomial fit correction, based on the secondary calibrations standards was used to correct for drifts in signal intensity.

Table 3. Instrument operating and data acquisition parameters

	Parameters
<b>Per Element Setting</b>	<b>Measured Wavelength (nm)</b>
B	249.772
Si	251.611
Al	394.401
Ca	616.217
Fe	259.940
<b>Common Conditions</b>	
Replicates	3
Pump Speed limit, (rpm)	10
Uptake time, (s)	30
Switch delay, (s)	28
Rinse time, (s)	30
Stabilization time, (s)	25
Number of Pixels	3
Calibration fit	Linear

## 4. Results and Discussion

### 4.1. Experiment 1

In experiment 1, 2 flux to sample ratios (5:1,10:1) were studied with samples of 1%, 6%, and 12% boric acid mixed with basalt powder. In the 5:1 ratio, it is seen that the sample powder amount was too small for the fusion technique, as the fusion cake was not homogenous and showed different colour patterns. The mixing color is also different from the 10:1 ratio. In *Figure 2*, the image shows the sample condition after fusion for 5:1 ratio sample.



*Figure 2. 5:1 ratio samples after fusion step*

The 10:1 ratio fusion cake were a different color than the 5:1 ratio. *Figure 3*, shows the 10:1 sample fusion cake after the fusion step. It was evident that the 10:1 flux ratio was sufficient to ensure full reaction between sample and flux, producing a uniform fusion cake.



*Figure 3. 10:1 Rratio sample after fusion step*

For the first experiment Si and B concentrations in the dissolution liquids were measured. Si is the main constituent of basalt and its recovery serves as a merit of dissolution efficiency. Analysis of dissolution liquids from the experiments revealed that in 10:1 ratio sample solution from the first dissolution step (after addition of water and concentrated  $\text{HNO}_3$ ), boron concentration was in the expected range but was greatly underestimated in liquids from the second dissolution step (after addition of 100 ml of 2%  $\text{HNO}_3$ ). Concentrations of Si from the 10:1 ratio sample however, exhibited a reversed pattern where 1-st dissolution liquids showed

low concentration values and 2-nd dissolution step samples exhibited expected concentration values. All solutions of 5:1 ratio sample exhibited B concentration values in the expected range but the Si was greatly underestimated, showing that the basalt had not fully reacted with the  $\text{Na}_2\text{O}_2$ . For 10:1 ratio samples, combining the B concentration from 1-st dissolution step and Si concentration from 2-nd dissolution step the Si to B ratios were close to the expected values. These results revealed that 5:1 ratio was unsuitable and 10:1 showed better compatibility but there were unknown issues with chemical stability of B and Si. For full dissolution of Si, a larger dissolving volume (2-nd dissolution step) is needed but B loss was unexpected and could be connected to the choice of dissolving acids.

#### **4.2. Experiment 2**

In second experiment flux to sample ratio 10:1 were analyzed with natural basalt powder (without mixing with boric acid), and 6%, and 12% boric acid mixed with basalt powder. Si and B concentrations in the dissolution liquids were measured. The determined recovery rates for Si and B relative to the concentrations measured by XRF are shown in Table 3. For samples with boric acid addition, chemical composition was calculated based on the weights of mixed  $\text{H}_3\text{BO}_4$  and basalt. Chemical composition of the natural basalt is provided in *Annex 1*.

In 10:1 ratio samples solution from the first dissolution step after addition of concentrated HCl a solid white precipitate was formed which was the result of super saturation in respect to NaCl and its precipitation. During the 2<sup>nd</sup> dissolution step (after addition of 100 ml of 2%  $\text{HNO}_3$ ) the precipitate was fully re-dissolved.

The recovery for Si and B in *Table 3* show that use of HCl gave better recovery than  $\text{HNO}_3$  for both boron and silicon in case of all sample materials and that the recoveries were better from solutions of the 2-nd dissolution step. When using HCl in the first dissolution step in experiment 2 the formation of visible colloidal phase after second dissolution step was also lower than with  $\text{HNO}_3$ . The formation of colloidal silica phases has been documented by other authors (Cai et al., 2021).

For experiment 2 the  $\text{Na}_2\text{O}_2$  was found to have been ground sub optimally. The ground material exhibited unbroken granules, which also created some homogeneity issues with the sample powder and  $\text{Na}_2\text{O}_2$  when they were mixed together. It can be also a reason for getting lower recovery for Si and B during the second experiment.

The results revealed that using HCl is more suitable than  $\text{HNO}_3$  for both recovery and formation of colloidal phase during the dissolution steps and that 2-nd dissolution liquids should be used

Table 3. Recovery % of samples from HCl and HNO<sub>3</sub> acid digestion

Samples	Dissolution step	Ratio	Digested by	Si Recovery	B Recovery
Natural Basalt powder	1-st dissolution	10:1	Concentrated HNO <sub>3</sub>	72%	-
Natural Basalt powder	2-nd dissolution	10:1	Concentrated HNO <sub>3</sub>	80%	-
Natural Basalt powder	1-st dissolution	10:1	Concentrated HCl	77%	-
Natural Basalt powder	2-nd dissolution	10:1	Concentrated HCl	85%	-
Natural basalt mixed with Boric acid (6%)	1-st dissolution	10:1	Concentrated HNO <sub>3</sub>	71%	56%
Natural basalt mixed with Boric acid (6%)	2-nd dissolution	10:1	Concentrated HNO <sub>3</sub>	77%	56%
Natural basalt mixed with Boric acid (6%)	1-st dissolution	10:1	Concentrated HCl	76%	82%
Natural basalt mixed with Boric acid (6%)	2-nd dissolution	10:1	Concentrated HCl	91%	72%
Natural basalt mixed with Boric acid (12%)	1-st dissolution	10:1	Concentrated HNO <sub>3</sub>	76%	59%
Natural basalt mixed with Boric acid (12%)	2-nd dissolution	10:1	Concentrated HNO <sub>3</sub>	84%	58%
Natural basalt mixed with Boric acid (12%)	1-st dissolution	10:1	Concentrated HCl	72%	55%
Natural basalt mixed with Boric acid (12%)	2-nd dissolution	10:1	Concentrated HCl	85%	66%



### 4.3 Experiment 3

In experiment 3, same samples and acid were used as in experiment 2 but the sample amount was increased to 0.2 g while the flux to sample ratio remained as 10:1. Only second dissolution liquids were analyzed. In experiment 3 more elements were added to the analyte list. As the formation of colloidal material that was observed in previous experiments could cause losses of silicon. Other main constituents of basalt were analyzed to verify full dissolution of the material. For that reason,  $\text{Fe}_2\text{O}_3$ ,  $\text{CaO}$ ,  $\text{Al}_2\text{O}_3$  were also quantified as they are more stable in the solution phase and there should not be any losses during the analysis. 2<sup>nd</sup> dissolution samples solutions of 2<sup>nd</sup> experiment (0.1 g sample mass) were also reanalyzed.

The recovery chart for experiment 2 and 3 2<sup>nd</sup> dissolution samples is given in [Table 4](#). The second experiment samples that were re-run gave better recovery for Si and B than in the previous experiment. As the recovery trends between samples were similar in both analysis it is likely, that there was some sort of systematic bias in the experiment 2 analysis, due to sample preparation. Similarly, to experiment 2, HCl based sample dissolution gave better recoveries across all analytes when compared to  $\text{HNO}_3$  counterparts. The recovery of most analytes was consistently better in experiments with 0.2 g sample when compared to 0.1 g sample mass, with some exceptions in  $\text{SiO}_2$  recovery of  $\text{HNO}_3$  based samples. Increased digestion efficiency in the case of 0.2 g sample mass could be due to the fine powder form of  $\text{Na}_2\text{O}_2$  as more emphasis was given to fine milling of  $\text{Na}_2\text{O}_2$  and homogenization of the mixed powders in crucibles, prior to fluxing. Smaller grainsize of  $\text{Na}_2\text{O}_2$  and thorough mixing between the sample and the powdered reagent ensure better reaction chemistry during fluxing.

It was confirmed that HCl is better suited for dissolution of the fluxed samples. Sample mass of 0.2 g provided recovery of all elements within 7% (mostly 5%) range of expected values. Although 0.1 g sample mass samples from 2<sup>nd</sup> experiment gave lower recoveries, the cause could be connected to suboptimal fluxing conditions due to inhomogeneous mixing of the sample and the powdered reagent.

Table 4. Recovery % of samples from Experiment 3 and experiment 2

Samples	Sample mass g	Digested by	Recovery				
			Fe <sub>2</sub> O <sub>3</sub>	SiO <sub>2</sub>	CaO	H <sub>3</sub> BO <sub>3</sub>	Al <sub>2</sub> O <sub>3</sub>
Natural Basalt powder	0.2	Concentrated HNO <sub>3</sub>	94%	80%	100%	–	103%
Natural Basalt powder	0.1	Concentrated HNO <sub>3</sub>	88%	91%	97%	–	92%
Natural Basalt powder	0.2	Concentrated HCl	95%	96%	101%	–	99%
Natural Basalt powder	0.1	Concentrated HCl	92%	94%	100%	–	98%
Natural basalt Powder mixed with Boric acid (6%)	0.2	Concentrated HNO <sub>3</sub>	92%	82%	100%	103%	102%
Natural basalt Powder mixed with Boric acid (6%)	0.1	Concentrated HNO <sub>3</sub>	81%	85%	88%	93%	87%
Natural basalt powder mixed with Boric acid (6%)	0.2	Concentrated HCl	93%	95%	103%	100%	103%
Natural basalt powder mixed with Boric acid (6%)	0.1	Concentrated HCl	95%	98%	102%	108%	99%
Natural basalt powder mixed with Boric acid (12%)	0.2	Concentrated HNO <sub>3</sub>	97%	88%	108%	106%	104%
Natural basalt powder mixed with Boric acid (12%)	0.1	Concentrated HNO <sub>3</sub>	89%	93%	94%	101%	93%
Natural basalt powder mixed with Boric acid (12%)	0.2	Concentrated HCl	96%	98%	102%	107%	103%
Natural basalt Powder mixed with Boric acid (12%)	0.1	Concentrated HCl	91%	94%	97%	103%	98%

#### 4.4 Experiment 4

In experiment 4 commercial samples of Chernvitsi and Bavoma basalt fiber doped with  $B_2O_3$  were analyzed. According to Chernvitsi supplier, one sample contains 12% of  $B_2O_3$  and the other contains 6% of  $B_2O_3$ . According to Bavoma supplier their sample contains 12% of  $B_2O_3$ . Two different sample masses 0.2 g and 0.1 g were used for these samples with 10:1 flux: sample ratio. Measured concentration information for all samples is provided in Annex 2.

Chernvitsi 6%  $B_2O_3$  doped basalt fiber sample mean values and standard deviations of two replicates for each mass (0.2 g and 0.1 g) are presented in *Figure 4*.

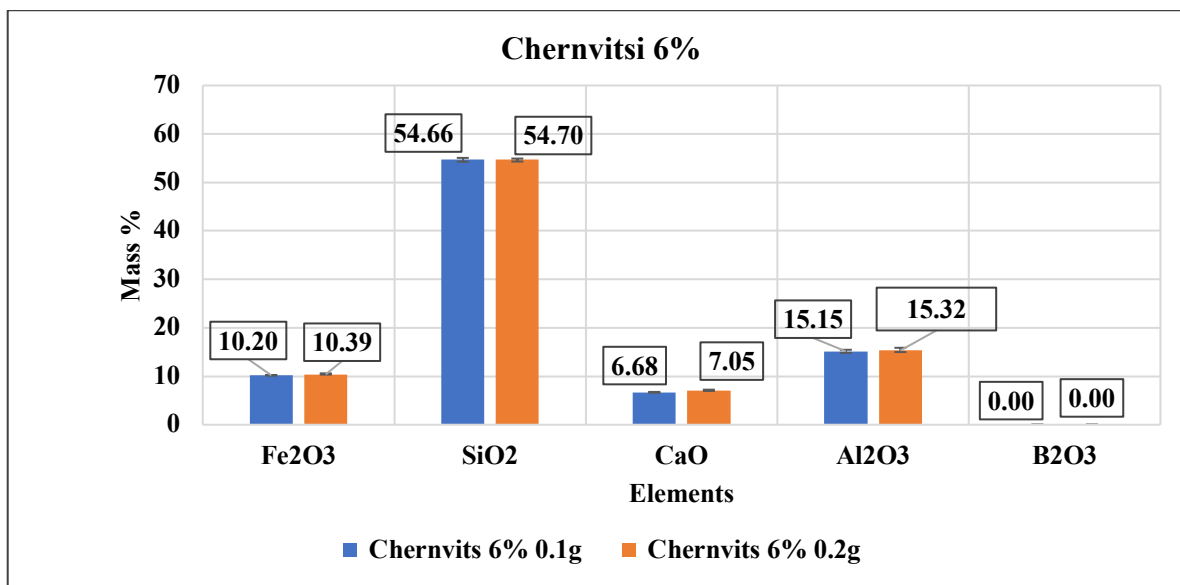


*Figure 4. Average concentration (wt%) of elements in Chernvitsi 6% by MP-AES*

*Figure 4* shows that the mass percentage of  $B_2O_3$  in the Chernvitsi 6 % sample is 0 % for both masses (0.2 g and 0.1 g). Concentrations of other analytes were comparable between different sample masses and were on average 10.29%  $Fe_2O_3$ , 54.68 %  $SiO_2$ , 6.86%  $CaO$ , and 15.23%  $Al_2O_3$ .

For Chernvitsi 12%  $B_2O_3$ -doped basalt fiber sample mean values and standard deviations of two replicates for each mass (0.2 g and 0.1 g) are presented in *Figure 5*.

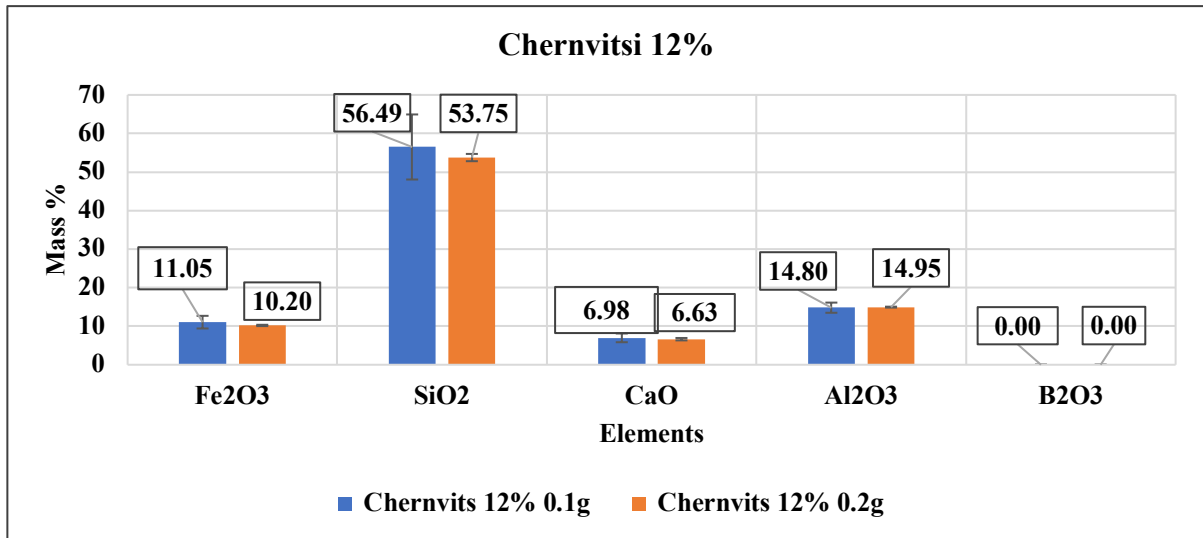


Figure 5. Average concentration (wt%) of elements in Chernvitsi 12% by MP-AES

Figure 5 shows that the sample, which the provider claims to contain 12% boron in the form of boric acid, actually does not contain any. Concentrations of other analytes in 0.2 g sample showed standard deviation of around 2%, but in the case of 0.1 g sample the standard deviation was 15% and the average concentrations of Fe<sub>2</sub>O<sub>3</sub>, SiO<sub>2</sub> and CaO were 5-8% higher, relative to 0.2 g sample. The cause of this variability could not be determined.

However, if we compare the average concentration of Chernvitsi 6% (all sample masses) and Chernvitsi 12% (0.2 g sample mass) (Figure 6) the measured concentrations are within standard deviation values and show that the material is with the same composition and doping with boron has not been successful.

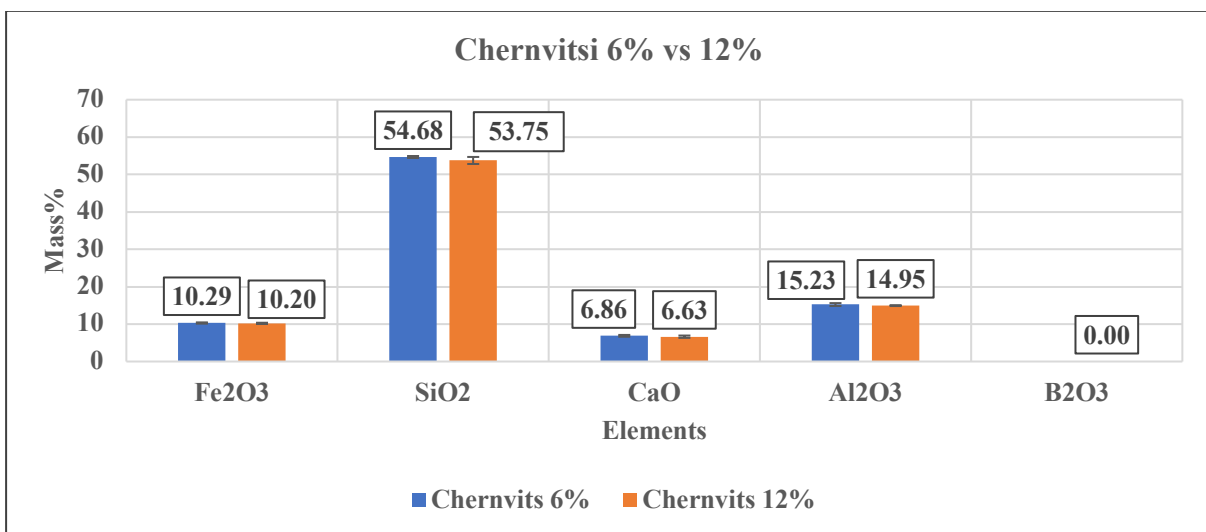
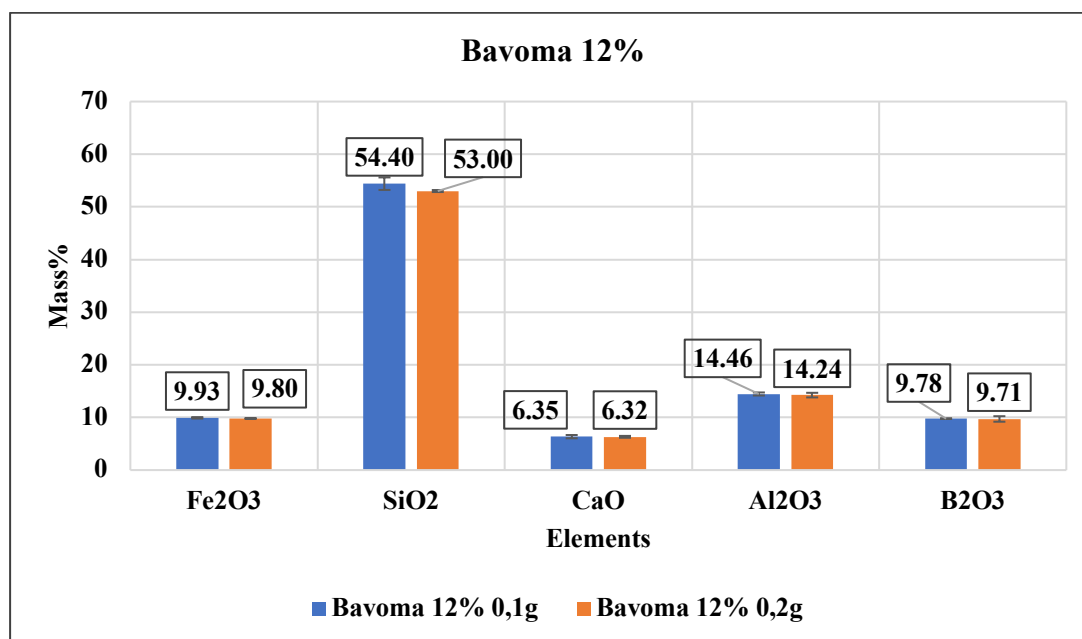


Figure 6. Average concentration (wt%) of elements in Chernvitsi 6% (all sample masses) and Chernvitsi 12% (0.2 g) by MP-AES

For Bavoma 12% B<sub>2</sub>O<sub>3</sub>-doped basalt fiber sample mean values and standard deviations of two replicate measurements for each sample mass (0.2 g and 0.1 g) are presented in *Figure 7*.



*Figure 7. Average concentration (wt%) of elements in Bavoma 12% by MP-AES*

For the Bavoma sample, which the provider claims to contain 12 percent B<sub>2</sub>O<sub>3</sub> average concentration of 9.74% B<sub>2</sub>O<sub>3</sub> was measured, which is far closer to the supplier's claims of 12 % than the Chervitsi samples. Concentrations of other analytes were comparable between different sample masses and were on average 9.86% Fe<sub>2</sub>O<sub>3</sub>, 53.7 % SiO<sub>2</sub>, 6.33 % CaO, and 14.35 % Al<sub>2</sub>O<sub>3</sub>.

It can be concluded from the above analysis that neither of the Chervitsi samples had any B<sub>2</sub>O<sub>3</sub> present in their samples, highlighting the need to validate the concentrations of such materials before application.

#### **4.4 Experiment 5**

In experiment 5, two samples of Bavoma with expected B<sub>2</sub>O<sub>3</sub> concentrations of 6% and 12% that had been milled by unknown means for another project were analyzed. Measured concentration information from MP-AES and ICP-MS measurements for all samples is provided in Annex 3.

Bavoma 6% B<sub>2</sub>O<sub>3</sub>-doped basalt fiber sample mean values and standard deviations of 3 replicate measurements for each sample mass (0.2 g and 0.1 g) are presented in *Figure 8*.

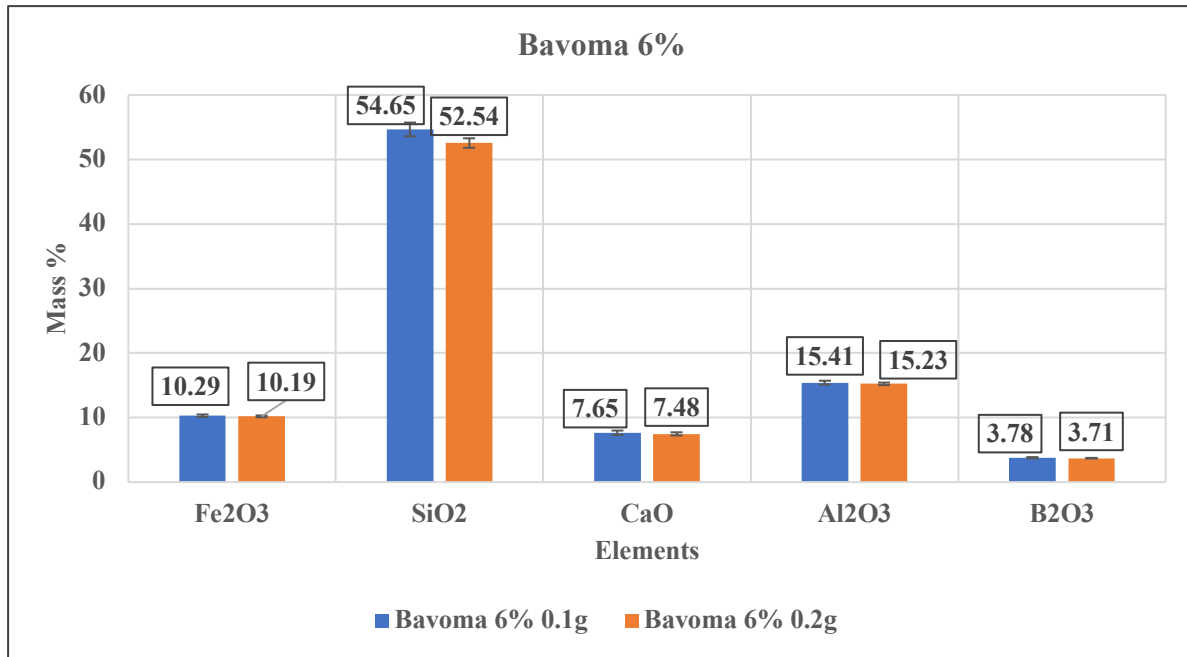


Figure 8, Average concentration (wt%) of elements in Bavoma 6% by MP-AES

From Figure 8 it can be seen that the mass percentage of B<sub>2</sub>O<sub>3</sub> in sample is 3.78% for 0.1 g of mass sample and 3.71% for 0.2 g of mass sample with an average of 3.74% across all measurements. As per the supplier, the expected concentration should be near 6%. Concentrations of other analytes were comparable between different sample masses and were on average 10.24% Fe<sub>2</sub>O<sub>3</sub>, 53.6 % SiO<sub>2</sub>, 7.56 % CaO, and 15.32 % Al<sub>2</sub>O<sub>3</sub>. Although within the range of standard deviation, the measured SiO<sub>2</sub> concentration in 0.2 g samples was on average 2 wt% lower than in 0.1 g samples.

Bavoma 12% B<sub>2</sub>O<sub>3</sub>-doped basalt fiber sample mean values and standard deviations of 3 replicate measurements for each sample mass (0.2 g and 0.1 g) are presented in Figure 9.

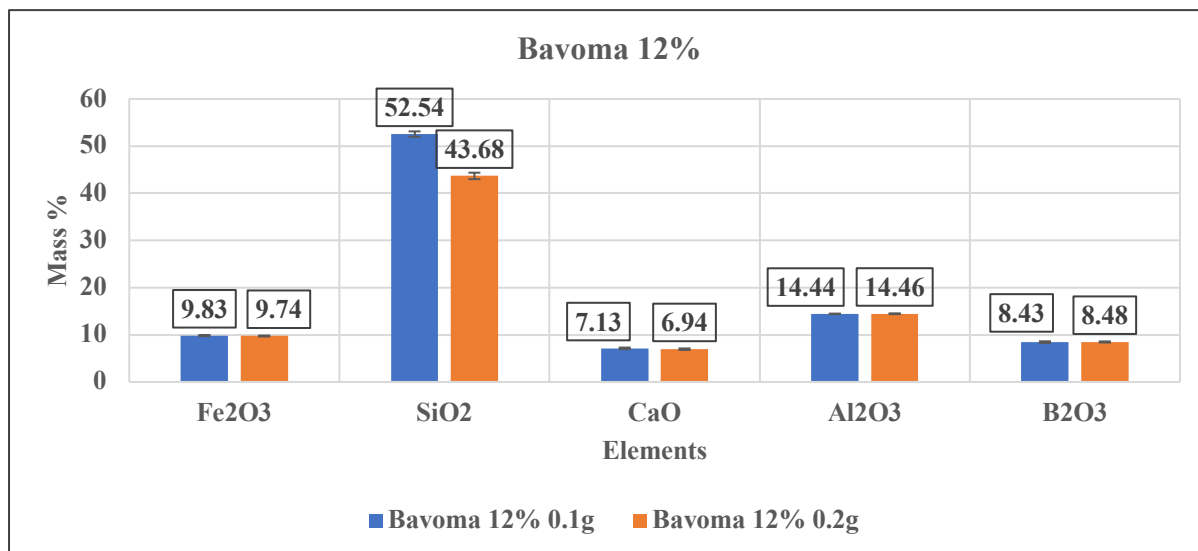


Figure 9. Average concentration (wt%) of elements in Bavoma 12% by MP-AES

From Figure 9 it can be seen that the mass percentage of B<sub>2</sub>O<sub>3</sub> in sample is 8.43% for 0.1 g of mass sample and 8.48% for 0.2 g of mass sample with an average of 8.45% across all measurements. Concentrations of Fe<sub>2</sub>O<sub>3</sub>, CaO and Al<sub>2</sub>O<sub>3</sub> were comparable between different sample masses, within the standard deviation range and on average 9.79 %, 7.03 % and 14.45% respectively. There is however a marked difference between the measured SiO<sub>2</sub> concentrations of 0.1 g and 0.2 g samples. The lower measured concentrations in 0.2 g sample is likely caused by formation and precipitation of colloidal silica phase. As the same phenomenon but to a lower extent was also observed with Bavoma 6% samples, it could be due to insufficient final sample volume as the concentration of dissolved Si in 0.2 g samples is almost 2 times higher than in the 2-nd dissolution liquids of 0.1 g samples. The average concentrations of Fe<sub>2</sub>O<sub>3</sub> and Al<sub>2</sub>O<sub>3</sub> of both sample masses and SiO<sub>2</sub> of 0.2 g sample were within standard deviation range of Bavoma 12% samples analyzed in experiment 4. The measured B<sub>2</sub>O<sub>3</sub> concentration was 1.29 wt% higher in the results from experiment 4. As other main constituents were found in similar concentration, possible boron contamination during sample preparation cannot be ruled out and could have arisen from milling with ethanol.

To validate that the calibration of MP-AES instrument is correct and the results are accurate, the same sample solutions were also analyzed using Agilent 8800 ICP-MS. Figure 10 and Figure 11 show the comparison between the average concentrations derived from MP-AES and ICP-MS measurements. SiO<sub>2</sub> was not quantified as it could not be determined during the analytical run with ICP-MS. For ICP-MS analysis the samples were diluted to an optimal B

concentration in the final solution, and due to that, the concentration of Fe, Ca and Al were out of calibration range. The analytical conditions were also suboptimal for the determination of high concentrations of analytes and due to that, the concentration values thus obtained must be considered with reservation.

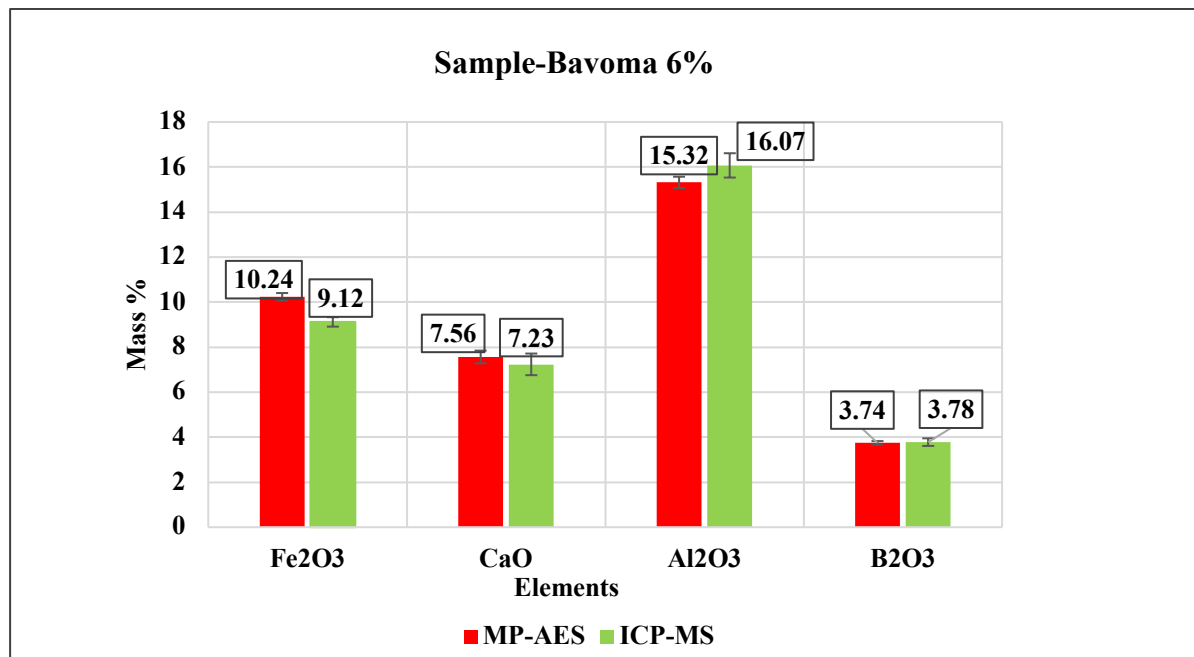


Figure 10. Average concentration (wt%) of elements in Bavoma 6% by MP-AES and ICP-MS

For Bavoma 6% sample (Figure 10) the result from MP-AES and ICP-MS correlate well with each-other and especially so in the case of B<sub>2</sub>O<sub>3</sub> with average concentrations of 3.74% and 3.78% respectively. Only Fe<sub>2</sub>O<sub>3</sub> concentrations did not overlap within the standard deviation range and were 1.12wt% lower than MP-AES based results. Same trend is true for CaO but for Al<sub>2</sub>O<sub>3</sub>, ICP-MS based concentrations were higher.

For Bavoma 12% sample (Figure 11) the result from MP-AES and ICP-MS measurements don't correlate as well as for Bavoma 6% but best agreement can be seen for B<sub>2</sub>O<sub>3</sub> values with 8.45% and 7.88% corresponding to MP-AES and ICP-MS respectively. Fe<sub>2</sub>O<sub>3</sub> and CaO concentrations were higher for MP-AES based measurements and lower for Al<sub>2</sub>O<sub>3</sub> measurements when compared to ICP-MS based values, exhibiting a similar trend to Bavoma 6% samples but to a greater degree.



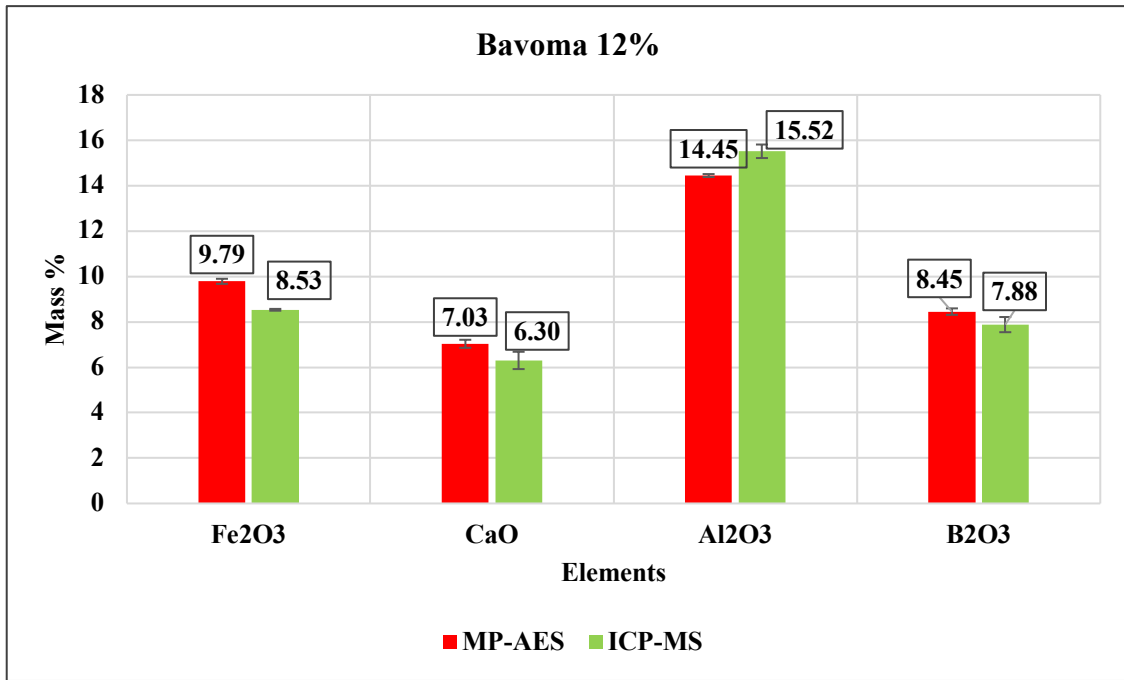


Figure 11. Average concentration (wt%) of elements in Bavoma 12% by MP-AES and ICP-MS

#### 4.5. XRF Analysis

The samples analyzed with XRF were natural basalt mixed with boric acid (labels BsltX% H<sub>3</sub>BO<sub>3</sub> EZ30) or lithium borate (labels LiBX% B<sub>2</sub>O<sub>3</sub> ez30) and the commercial samples which are labeled in the spectrum on Figure 12 as Ba 6% (Bavoma 6%) and MK 6%, MK12% (Chernvitsi 6% and 12%). Comparison of spectrums reveal a very distinct difference. The boron K $\alpha$  peak intensity difference between crystalline and x-ray amorphous boron phases used for doping was observed. The H<sub>3</sub>BO<sub>3</sub> (boric acid) is a crystalline phase and lithium borate (as LiTB/LiMB mix) is an X-ray amorphous phase. Although both additives produce a higher signal with increasing concentration, the signal intensity for boric acid-based mixes is much more intense, highlighting matrix effects in XRF measurements.

The natural basalt spectrum (Bslt0% H<sub>3</sub>BO<sub>3</sub> EZ30) shows higher peak intensity than the commercial fiber samples MK6% and MK12% (Chernvitsi 6% and 12%), confirming the findings from MP-AES measurements that no boron is present in those samples. As the signal intensities of the MK samples were similar it shows that there is no distinct difference in the boron concentration between these samples. The higher signal intensity of the natural basalt when compared to Chernvitsi samples can arise from differences in the composition of the basalts and the intensity of spectral overlaps in the boron K $\alpha$  region.

The Ba 6% (Bavoma 6%) sample showed a difference spectrum than the MK (Chernvitsi) samples. The signal intensity shows that boron is present in the sample and when compared to LiTB/LiMB doped basalt spectrums the signal of the Bavoma sample lies between the 8% and 12% B<sub>2</sub>O<sub>3</sub> (LiB8/12% B<sub>2</sub>O<sub>3</sub> ez30) containing doped basalt sample spectrums, indicating a concentration within that range (8-12% B<sub>2</sub>O<sub>3</sub>). The concentration value from dissolution experiments however was below 4%.

The results show that the chemical form of boron (crystalline or x-ray amorphous) has a direct impact on the signal intensity. Although doping of natural basalt with LiTB/LiMB produces a more similar spectrum to the basalt fiber samples, there are systematic differences. These could be caused by differences in concentration of other major or trace constituents of the natural basalt and commercial basalt fibers or the chemical environment of boron in the sample. If basalt fibers from the same producer without boron addition could be obtained, doping with x-ray amorphous boron substrate could be used to create calibration standards but this will need further validation.

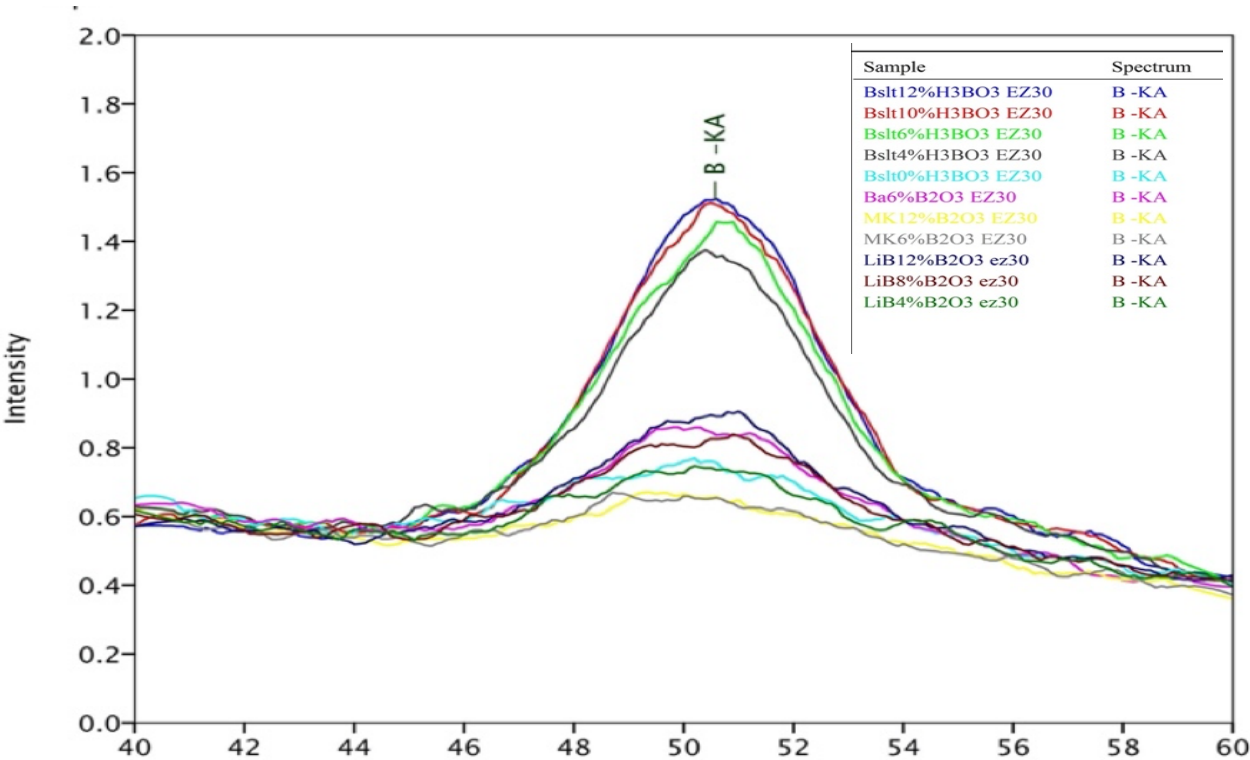


Figure 12. XRF spectrums of basalt powder samples and samples from suppliers Bavoma and Chernvitsi.

## 5. Conclusion

Experiments with different dissolution acids and various sample masses and flux to sample ratios revealed that the use of HCl is a better option than HNO<sub>3</sub> for dissolution of Na<sub>2</sub>O<sub>2</sub> based flux cakes. HCl based dissolution is more complete, less chances of colloidal formation and the recovery of both boron and silica is better. When using 10:1 flux to sample ratio and 0.1 g or 0.2 g of sample, experiments with the real samples yielded comparable results. Recovery of boron was found to be in an acceptable range for boric acid doped natural basalt samples. Also, silica content was measured. Si is the main constituent of basalts and its recovery highlights the dissolution efficiency of experimental work. However, Si stability and formation of colloidal silica phase could be observed in samples that were dissolved using HNO<sub>3</sub> and also occurred to a smaller degree in samples dissolved using HCl. This interferes with complete Si dissolution and affect measurement quality. The formation of colloidal Si can be reduced by increasing liquid volume at the second dissolution step. Comparative measurements with ICP-MS and MP-AES confirmed the suitability of MP-AES method for the determination of boron. Experiments with basalt fibers revealed that fibers produced by Chervitsi did not contain any boron, highlighting the importance of conducting quality control measurements of such material, prior to its application. XRF analysis of boron doped natural basalt samples and basalt boron fibers is in accordance with MP-AES results, indicating no boron in Chervitsi samples. Natural basalt used in experiments reveal higher B concentration than Chervitsi basalt boron fibers, which may be due to compositional variations in natural basalts used in both cases. Notable differences could also be observed in XRF spectra B-K $\alpha$  intensities between crystalline (H<sub>3</sub>BO<sub>3</sub> - boric acid) and x-ray amorphous (LiTB/LiMB mix) boron phases used for doping natural basalt samples. The signal intensity for boric acid-based mixes is much more intense, highlighting matrix effects in XRF measurements.

## 6. Summary

Use of boron doped basalt fibers as an additive to concrete can enhance mechanical properties and improve neutron shielding characteristics of concretes used in management of hazardous and radioactive materials. To evaluate the shielding capabilities of concrete, which is a function of boron in basalt boron fibers, it is necessary to identify the amount of boron oxide in basalt boron fiber. Quality check is necessary, since the chemical composition of (commercial) products may deviate from its product declaration. Determination of the boron concentration in such fiber compounds can however be difficult and costly.

The aim of the present thesis was to develop a method to determine the boron content in boron doped basalt fibers. Two types of samples were investigated: natural basalt powders doped with  $H_3BO_4$ , which were used for method development and then this developed method was applied to basalt fiber samples from two different fiber producers.

Alkaline fusion with  $Na_2O_2$  was used as the dissolution method and the use of HCl and  $HNO_3$  for dissolving the fusion residue were investigated. It was found that the use of HCl provided better results than the use of  $HNO_3$ . It was also observed, that if the  $Na_2O_2$  is not grounded properly it can affect the final digestion efficiency and a flux to sample ratio of 10:1 was found to be suitable at sample mass of 0.1 and 0.2 g.

Analysis of dissolution liquids was performed with MP-AES and the suitability of the analytical method was checked with ICP-MS and experiments were also conducted using XRF.

Comparative measurements with ICP-MS and MP-AES confirmed the suitability of MP-AES method for the determination of boron. Experiments with basalt fibers revealed that fibers from one commercial producer did not contain any boron, highlighting the importance of conducting quality control measurements of such material, prior to its application. XRF analysis of boron doped natural basalt samples revealed that the crystal structure of boron containing phases has a severe impact on the peak shape of B- $K\alpha$  and it is difficult to determine the boron concentration in the fiber sample with this method.

To conclude, combination of alkali fusion with  $Na_2O_2$  and analysis with MP-AES was shown to be an effective method for determination of boron in basalt fibers.

## 7. Acknowledgements

This work was part of ICONDE project, supported by the European Economic Area Grants, EEA-RESEARCH-165.

## 8. Kokkuvõte

Booriga rikastatud basaltfiibri kasutamine eribetonide tootmises võimaldab samaaegselt parandada betooni tugevusomadusi ja boori lisand fiibris pakub varjestusomadusi kõrgradioaktiivsetest materjalidest pärineva neutronkiirguse vastu. Selleks, et hinnata fiiberlisandiga betooni varjestusomadusi on oluline teada boori sisaldust fiibris. Selle määramine on praktikas aga keeruline või kallis.

Käesoleva magistritöö eesmärgiks oli töötada välja meetodika boori määramiseks basaltfiibrites. Selleks uurisin kahte tüüpi materjale: meetodi välja töötamiseks kasutasin  $H_3BO_4$  lisandiga pulbriks jahvatatud basalti ning välja töötatud meetodika rakendasin kahe erineva tootja poolt valmistatud basaltfiibritel.

Proovide mineraliseerumiseks kasutasin  $Na_2O_2$ -l baseeruvat leeliselisist sulandamist ning protsessi käigus tekkinud sulandi lahustamist uurisin kontsentreeritud  $HCl$  ja  $HNO_3$  kasutades. Selgus, et  $HCl$  kasutamine annab paremaid tulemusi kui  $HNO_3$ . Ning kui  $Na_2O_2$  ei ole enne fusiooni reaktsiooni piisavalt hästi jahvatatud, võib see mõjutada lahustamise efektiivust ja optimaalne on kasutada lahustamisel  $Na_2O_2$  ning proov suhet 10:1, mis töötab nii 0.1 g kui 0.2 g proovimassi korral.

Lahustamise käigus tekkinud lahuseid analüüsisime kasutades MP-AES meetodikat ning selle tulemusi kontrollisime lisaks ICP-MS analüüsiga. Samuti analüüsisime osade proovide keemilist koostist XRF spektrometriga. ICP-MS ja MP-AES võrdlusmõõtmiste tulemused kinnitasid MP-AES-i sobivust boori analüüsimiseks uuritud proovidest. Basaltfiibritega teostatud eksperimentidest selgus, et ühe tootja poolt valmistatud, väidetavalt boori lisandiga, basaltfiibrid ei sisaldanud üldse boori. See tulemus näitab ilmekalt vajadust kontrollida fiibrite tegelikku boori sisaldust enne sellise toodangu kasutust kõrgete kvaliteedinõuetega rakendustes. Erineva, nii kristallilise kui amorfse boori lisanditega rikastatud loodusliku basaldi proovide XRF mõõtmistest selgus, et boori lisandi kristalliinsus mõjutab tugevalt B- $K\alpha$  tipu intensiivsust, mis mõjutab B kvantifitseerimist ja seega muudab suhteliselt lihtsa XRF meetodi kasutuse basaltfiibrite analüüsimisel keerukamaks.

Kokkuvõtvalt võib väita, et boori sisaldavate basaltfiibrite lahustamine  $Na_2O_2$ -l baseeruva leeliselise sulandamise kaudu, sulandi lahustamine ja sellele järgnev analüüs MP-AES meetodikat rakendades on sobilik meetod määramaks boori sisaldust neis materjalides.

## 8. References

- Acharya, R. Prompt gamma-ray neutron activation analysis methodology for determination of boron from trace to major contents. *Journal of radioanalytical and nuclear chemistry*. (2009) 291-294.
- Al-Warthan, A. A., Al-Showiman, S. S., Al-Tamrah, S. A., & Baosman, A. A. Spectrophotometric determination of boron in dates of some cultivars grown in Saudi Arabia. *Journal of AOAC International*. (1993) 601-603.
- Ammann, A. A. Inductively coupled plasma mass spectrometry (ICP MS): a versatile tool. *Journal of mass spectrometry*. (2007) 419-427.
- Aramendía, M., Rello, L., Bérail, S., Donnard, A., Pécheyran, C., & Resano, M. Direct analysis of dried blood spots by femtosecond-laser ablation-inductively coupled plasma-mass spectrometry. *Royal Society of Chemistry*. (2015) 296-309.
- Brown, R. N. Techniques for boron determination and their application to the analysis of plant and soil samples. *Springer*. (1997) 15-33.
- Burguera, M., Burguera, J. L., Rondón, C., & Carrero, P. Determination of boron in blood, urine and bone by electrothermal atomic absorption spectrometry using zirconium and citric acid as modifiers. *science Direct* . (2001) 1845-1857.
- Cai, Y., Rasbury, E. T., Wooton, K. M., Jiang, X., & Wang, D. Rapid boron isotope and concentration measurements of silicate geological reference materials dissolved through sodium peroxide sintering. *ournal of Analytical Atomic Spectrometry*. (2021) 2153-2163.
- Carrero, P., Malavé, A., Rojas, E., Rondón, C., de Peña, Y. P., Burguera, J. L., & Burguera, M. On-line generation and hydrolysis of methyl borate for the spectrophotometric determination of boron in soil and plants with azomethine-H. *Science direct* (2005) 374-381.
- Chen-Mayer, H. H., Mackey, E. A., Paul, R. L., & Mildner, D. F. R. Quantitative prompt gamma analysis using a focused cold neutron beam. *ournal of Radioanalytical and Nuclear Chemistry*. (2000) 391-397.
- Copley, J. R. D., & Stone, C. A. Neutron scattering and its effect on reaction rates in neutron absorption experiments. *Nuclear Instruments and Methods in Physics Research Section A: Accelerators, Spectrometers, Detectors and Associated Equipment*, 281(3) (1989) 593-604.
- Dai, S., Song, W., Zhao, L., Li, X., Hower, J. C., Ward, C. R., & Li, Q. Determination of Boron in Coal Using Closed-Vessel Microwave Digestion and Inductively Coupled Plasma Mass Spectrometry (ICPMS). *Academia*. (2014) 4517-4522.
- de Lima, B. B., Conte, R. A., & Nunes, C. A. Analysis of nickel–niobium alloys by inductively coupled plasma optical emission spectrometry. *Science Direct*. (2003) 89-93.
- DeFrancesco & Coca, A. Boron chemistry: an overview. *Boron reagents in synthesis*. (2016) 1-25.

Eyüp Zorla, Cagatay Ipbüker, Alex Biland, Madis Kiisk, Sergei Kovaljov, Alan H. Tkaczyk, Volodymyr Gulik. Radiation shielding properties of high performance concrete reinforced with basalt fibers infused with natural and enriched boron. *Nuclear Engineering and Design*, 313 (2017) 306-308.

G. S. Banuelos, G. Cardon, T. Pflaum & S. Akohoue. Comparison of dry ashing and wet acid digestion on the determination of boron in plant tissue. *Communications in Soil Science and Plant Analysis*. (1992) 2383-2397.

Hu, W.D. Determination of boron in high-purity silica using direct current plasma emission spectrometry. *Analytica chimica acta*, 245 . (1991) 207-209.

Jeyakumar, S., Raut, V. V., & Ramakumar, K. L. Simultaneous determination of trace amounts of borate, chloride and fluoride in nuclear fuels employing ion chromatography (IC) after their extraction by pyrohydrolysis. *Science direct*. (2008) 1246-1251.

Kleinhanns, I. C., Kreissig, K., Kamber, B. S., Meisel, T., Nägler, T. F., & Kramers, J. D. Combined chemical separation of Lu, Hf, Sm, Nd, and REEs from a single rock digest: precise and accurate isotope determinations of Lu– Hf and Sm– Nd using multicollector-ICPMS. *Academia*, (2002) 67-73.

Krejčová, A., & Černohorský, T. The determination of boron in tea and coffee by ICP–AES method. *Science Direct*. (2003) 303-308.

Li-Qiang, X., & Zhu, R. Determination of boron in soils by sequential scanning ICP-AES using side line indexing method. *Fresenius' Zeitschrift für analytische Chemie*, 534-538. Lu, G., Li, X., & Deng, Y. (1994). Polarographic determination of trace boron in foods. *Food chemistry*. (1986) 91-93.

Meisel, T., Schöner, N., Paliulionyte, V., & Kahr, E. Determination of rare earth elements, CHERNVITSI, Th, Zr, Hf, Nb and Ta in geological reference materials G-2, G-3, SCo-1 and WGB-1 by sodium peroxide sintering and inductively coupled plasma-mass spectrometry. *Geostandards Newsletter*. (2002) 26, 53-61.

Montesano, R. K. T. L., Matsumoto, K., Nakamura, T., & Orci, L. Identification of a fibroblast-derived epithelial morphogen as hepatocyte growth factor. *Sciencedirect*, 67(5) . (1991) 901-908.

Motomizu, S. & Oshima, M., & Jun, Z. Fluorimetric determination of boron with chromotropic acid by flow-injection analysis. *Analytica chimica acta*. (1991) 269-274.

N. BRACK, A. N. RIDER, B. HALSTEAD, P. J. PIRAMG. Surface modification of boron fibres for improved strength in composite materials . *VSP International Science Publishers*. (2005, May 14)

Nakamura, E., Ishikawa, T., Birck, J. L., & Allègre, C. J. Precise boron isotopic analysis of natural rock samples using a boron-mannitol complex. *Chemical Geology*. (1992) 193-204.

pez-García, I., Vinas, P., Romero-Romero, R., & Hernández-Córdoba, M. Preconcentration and determination of boron in milk, infant formula, and honey samples by solid phase extraction-electrothermal atomic absorption spectrometry. *Science Direct*. . (2009) 179-183.

Raaijmakers, C. P. Monitoring of blood-<sup>10</sup>B concentration for boron neutron capture therapy using prompt gamma-ray analysis. *Acta Oncologica*. (1994) 517-523.

Raja, S.W., Acharya, R. & Pujari, P.K. Application of PIGE method for quantification of total boron in neutron absorbers and shielding materials and isotopic composition in in-house prepared enriched boron carbide samples. *J Radioanal Nucl Chem*. (2020) 1359–1366.

Resano, M., Briceño, J., Aramendia, M., & Belarra, M. A. Solid sampling-graphite furnace atomic absorption spectrometry for the direct determination of boron in plant tissues. *Science Direct*. (2007) 214-222.

Richardson, S. D. Mass spectrometry in environmental sciences. *American Chemical Society* . (2001) 211-254.

Rietig, A., & Acker, J. Development and validation of a new method for the precise and accurate determination of trace elements in silicon by ICP-OES in high silicon matrices. *Journal of Analytical Atomic Spectrometry*. (2017) 322-333.

Sah, R. N., & Brown, P. H. (1997). Techniques for boron determination and their application to the analysis of plant and soil samples. *Springer*, 15-33.

Sanchez-Ramos, S., Bosch-Reig, F., Gimeno-Adelantado, J. V., Yusa-Marco, D. J., Domenech-Carbo, A., & Berja-Perez, J. A. Validation of a method for the determination of boron in ceramic materials by X-ray fluorescence spectrometry. *Spectrochimica Acta Part B: Atomic Spectroscopy*. (2000) 1669-1677.

SARICA, D. Y., & ERTAŞ, N. Flow injection analysis for boron determination by using methyl borate generation and flame atomic emission spectrometry. *Turkish Journal of Chemistry*. (2001) 305-310.

Song, S. G.). Recent developments in the medicinal chemistry of single boron atom-containing compounds. *Acta Pharmaceutica Sinica B*,. (2021) 3035-3059.

Sreenivasulu, V., Kumar, N. S., Dharmendra, V., Asif, M., Balaram, V., Zhengxu, H., & Zhen, Z. Determination of Boron, Phosphorus, and Molybdenum Content in Biosludge Samples by Microwave Plasma Atomic Emission Spectrometry (MP-AES). *Research gate* (2007).

Terekhova, A. M., Levchenko, Y. V., Matveeva, T. V., Borisov, I. S., & Chelmakov, I. A. Influence of boron enrichment in control rods on neutron-physical characteristics of the core of the reactor VVER. *IOP Conference Series: Materials Science and Engineering, Volume 487, The II International (XV Regional) Scientific Conference "Technogenic Systems and Environmental Risk" 19–20 April 2018, Kaluga Region, Russian Federation* IOP Publishing Ltd. (2019) pp. 1-8.

Tonarini, S., Pennisi, M., & Leeman, W. P. Precise boron isotopic analysis of complex silicate (rock) samples using alkali carbonate fusion and ion-exchange separation. *Chemical Geology*, 142 (1-2) (1997) 129-137.



Tu, K. L., Nghiem, L. D., & Chivas, A. R. Boron removal by reverse osmosis membranes in seawater desalination applications. *Science Direct*. (2010) 87-101.

van Sprang, H. A., & Bekkers, M. H. Determination of light elements using x-ray spectrometry. *Boron in glass. X-Ray Spectrometry*. (1998) 37-42.

Volynskii, A. B. Chemical modifiers in modern electrothermal atomic absorption spectrometry. *Springer* (2003) 905-921.

Vudagandla, S., Siva Kumar, N., Dharmendra, V., Asif, M., Balaram, V., Zhengxu, H., & Zhen, Z. Determination of boron, phosphorus, and molybdenum content in biosludge samples by microwave plasma atomic emission spectrometry (MP-AES) *MDPI*, 264 (2017).

Wood, J. & Nicholson, K. Determination of boron in environmental samples by ion-selective electrode: an evaluation. *Environmental Geochemistry and Health*, 87 (1994).

Woods, W.G. An introduction to boron: history, sources, uses, and chemistry. *Environmental health perspectives*. (1994) 5-11.

Yilmaz, A. E., Boncukcuoğlu, R., & Kocakerim, M. M . An empirical model for parameters affecting energy consumption in boron removal from boron-containing wastewaters by electrocoagulation. *Journal of hazardous Materials*. (2007) 101-107.

Yonezawa, C., & Wood, A. K. H. Prompt. gamma.-Ray Analysis for Boron with Cold and Thermal Neutron Guided Beams. *Analytical Chemistry*, 67(24) (1995) 4466-4470.

## 9. Annexes

### Annex 1

Chemical composition of natural basalt powder by XRF

Mass %										
Sample	SiO <sub>2</sub>	Al <sub>2</sub> O <sub>3</sub>	Fe <sub>2</sub> O <sub>3</sub>	TiO <sub>2</sub>	CaO	MgO	Na <sub>2</sub> O	K <sub>2</sub> O	MnO	SO <sub>3</sub>
Natural Basalt	46.16	13.61	12.90	2.65	11.19	6.51	2.30	0.50	0.23	0.16

### Annex 2

Data Used in Experiment 4 for graphical representation

Chernvitsi 12% (0.2g)

Mass %					
Sample	Fe <sub>2</sub> O <sub>3</sub>	SiO <sub>2</sub>	CaO	Al <sub>2</sub> O <sub>3</sub>	B <sub>2</sub> O <sub>3</sub>
12% Chernvits 0,2g	10.08	53.08	6.41	14.87	0
12% Chernvits 0.2g	10.32	54.42	6.85	15.03	0
Avg	10.20	53.75	6.63	14.95	0.00
Std.	0.17	0.94	0.31	0.12	0.00

Chernvitsi 12% (0.1g)

Mass %					
Sample	Fe <sub>2</sub> O <sub>3</sub>	SiO <sub>2</sub>	CaO	Al <sub>2</sub> O <sub>3</sub>	B <sub>2</sub> O <sub>3</sub>
12% Chernvits 0,1g	12.21	62.46	7.78	15.73	0
12% Chernvits 0.1g	9.89	50.53	6.18	13.87	0
Avg	11.05	56.49	6.98	14.80	0.00
Std.	1.64	8.44	1.13	1.32	0.00

Chernvitsi 6% (0.2g)

Mass %					
Sample	Fe <sub>2</sub> O <sub>3</sub>	SiO <sub>2</sub>	CaO	Al <sub>2</sub> O <sub>3</sub>	B <sub>2</sub> O <sub>3</sub>
6% Chernvits 0,2g	10.25	54.55	7.18	15.71	0
6% Chernvits 0,2g	10.53	54.85	6.92	14.92	0
Avg	10.39	54.70	7.05	15.32	0.00
Std.	0.20	0.22	0.18	0.56	0.00

Chernvitsi 6% (0.1g)

	Mass %				
Sample	Fe <sub>2</sub> O <sub>3</sub>	SiO <sub>2</sub>	CaO	Al <sub>2</sub> O <sub>3</sub>	B <sub>2</sub> O <sub>3</sub>
6% Chernvits 0,1g	10.23	54.94	6.74	15.37	0
6% Chernvits 0,1g	10.16	54.38	6.62	14.92	0
Avg	10.20	54.66	6.68	15.15	0,00
Std.	0.05	0.40	0.08	0.32	0,00

Bavoma 12% (0.2g)

	Mass %				
Sample	Fe <sub>2</sub> O <sub>3</sub>	SiO <sub>2</sub>	CaO	Al <sub>2</sub> O <sub>3</sub>	B <sub>2</sub> O <sub>3</sub>
12% Bavoma 0,2g	9.80	53.14	6.44	14.55	9.34
12% Bavoma 0,2g	9.79	52.87	6.19	13.93	10.08
Avg	9.80	53.00	6.32	14.24	9.71
Std.	0.01	0.19	0.18	0.44	0.52

Bavoma 12% (0.1g)

	Mass %				
Sample	Fe <sub>2</sub> O <sub>3</sub>	SiO <sub>2</sub>	CaO	Al <sub>2</sub> O <sub>3</sub>	B <sub>2</sub> O <sub>3</sub>
12% Bavoma 0,1g	10.02	55.24	6.57	14.66	9.74
12% Bavoma 0,1g	9.83	53.56	6.13	14.25	9.81
Avg	9.93	54.40	6.35	14.46	9.78
Std.	0.13	1.19	0.31	0.29	0.05

### *Annex3*

Data Used in Experiment 5 for graphical representation

Bavoma 6% (0.1g) measured value by MP-AES

	Mass %				
Sample	Fe <sub>2</sub> O <sub>3</sub>	SiO <sub>2</sub>	CaO	Al <sub>2</sub> O <sub>3</sub>	B <sub>2</sub> O <sub>3</sub>
6% Bavoma 0,1g	10.18	54.33	7.52	15.20	3.81
6% Bavoma 0,1g	10.51	55.83	8.03	15.76	3.67
Avg	10.35	55.08	7.78	15.48	3.74
Std.	0.24	1.07	0.37	0.40	0.10

Bavoma 6% (0.2g) measured values by MP-AES

Sample	Mass %				
	Fe <sub>2</sub> O <sub>3</sub>	SiO <sub>2</sub>	CaO	Al <sub>2</sub> O <sub>3</sub>	B <sub>2</sub> O <sub>3</sub>
6% Bavoma 0,2g	10.04	51.77	7.30	15.39	3.70
6% Bavoma 0,2g	10.33	53.23	7.75	15.01	3.66
Avg	10.19	52.50	7.53	15.20	3.68
Std.	0.20	1.03	0.32	0.27	0.03

Bavoma 12% (0.2g) measured values by MP-AES

Sample	Mass %				
	Fe <sub>2</sub> O <sub>3</sub>	SiO <sub>2</sub>	CaO	Al <sub>2</sub> O <sub>3</sub>	B <sub>2</sub> O <sub>3</sub>
12% Bavoma 0,2g	9.80	43.83	7.05	14.55	8.42
12% Bavoma 0,2g	9.63	42.93	6.75	14.38	8.40
12% Bavoma 0,2g	9.80	44.27	7.03	14.44	8.61
AVG	9.74	43.68	6.94	14.46	8.48
Std.	0.10	0.69	0.16	0.09	0.12

Bavoma 12% (0.1g) measured values by MP-AES

Sample	Mass %				
	Fe <sub>2</sub> O <sub>3</sub>	SiO <sub>2</sub>	CaO	Al <sub>2</sub> O <sub>3</sub>	B <sub>2</sub> O <sub>3</sub>
12% Bavoma 0,1g	9.84	52.22	7.12	14.48	8.26
12% Bavoma 0,1g	9.95	53.21	7.29	14.38	8.40
12% Bavoma 0,1g	9.71	52.20	6.97	14.45	8.63
AVG	9.83	52.54	7.13	14.44	8.43
Std.	0.12	0.58	0.16	0.05	0.19

Bavoma 6% and 12% sample (0.1 & 0.2g) measured values by ICP-MS

Sample	Mass %			
	B <sub>2</sub> O <sub>3</sub>	Al <sub>2</sub> O <sub>3</sub>	CaO	Fe <sub>2</sub> O <sub>3</sub>
6% Bavoma 0,1g	3.85	16.29	7.37	9.32
6% Bavoma 0,2g	3.58	15.45	6.70	8.89
6% Bavoma 0,1g	3.90	16.47	7.63	9.15
12% Bavoma 0,1g	7.94	15.23	6.10	8.49
12% Bavoma 0,2g	8.18	15.49	6.74	8.54
12% Bavoma 0,1g	7.52	15.83	6.07	8.57
BA 6% Avg	3.78	16.07	7.23	9.12
BA 6% Std.Dev	0.17	0.54	0.48	0.21
BA 12% Avg	7.88	15.52	6.30	8.53
BA 12% Std.Dev	0.33	0.30	0.38	0.04

## Non-exclusive licence to reproduce thesis and make thesis public

I, Faysal-Al-Mamun \_\_\_\_\_,

*(author's name)*

1. herewith grant the University of Tartu a free permit (non-exclusive licence) to:
2. reproduce, for the purpose of preservation, including for adding to the DSpace digital archives until the expiry of the term of copyright, and
3. I grant the University of Tartu a permit to make the thesis specified in point 1 available to the public via the web environment of the University of Tartu, including via the DSpace digital archives, under the Creative Commons licence CC BY NC ND 4.0, which allows, by giving appropriate credit to the author, to reproduce, distribute the work and communicate it to the public, and prohibits the creation of derivative works and any commercial use of the work until the expiry of the term of copyright.

Development of method for boron determination in basalt fibers

---

*(title of thesis)*

supervised by Päärn Paiste.

Riho Mõtlep

---

*(supervisor's name)*

4. I am aware of the fact that the author retains the rights specified in p. 1 and 2
5. I certify that granting the non-exclusive licence does not infringe other persons' intellectual property rights or rights arising from the personal data protection legislation.

*Faysal-Al-Mamun*  
24/05/2022

## INFORMATION SHEET

### Development of method for boron determination in basalt fibers

The main objective of the present thesis was to develop a method to determine the boron content of boron doped basalt fibers. Two types of samples were investigated: natural basalt powders doped with  $H_3BO_3$  were used for method development and the method was applied to basalt fiber samples from two different fiber producers.  $Na_2O_2$  based alkaline fusion with different sample masses and the use of HCl and  $HNO_3$  for dissolution of fusion residues was investigated. The results show that using 10:1 flux to sample ratio and HCl as dissolving acid allows for full digestion of sample and determination of boron content by MP-AES analysis. Results from the analysis of commercial basalt fibers revealed that fibers from one producer, contrary to the suppliers claim, did not contain any boron, highlighting the need for quality check and the development of method to do that.

Keywords: boron, basalt fiber, MP-AES

CERCS code: P300 Analytical chemistry

## INFOLEHT

### Basaltfiibritest boori määramise meetodika välja töötamine

Käesoleva magistridee peamiseks eesmärgiks oli välja töötada meetod boori sisalduse määramiseks booriga dopeeritud basaltfiibrites. Töö käigus kasutati meetodi välja töötamiseks  $H_3BO_4$ -ga dopeeritud looduslikku basalti ja meetodit rakendati kahe erineva tootja poolt valmistatud basaltfiibrite analüüsiks. Töö käigus uuriti  $Na_2O_2$  baseeruva leeliselise fusioonimeetodi efektiivsust eri proovimasside puhul ning HCl ja  $HNO_3$  sobivust fusioonitahkise lahustamisel. Tulemustest selgus, et kasutades  $Na_2O_2$ : proovi suhet 10:1 ja lahustamiseks HCl, saavutati proovi täielik lahustamine ning boori sisaldus lahusest määrati MP-AES'iga. Basaltfiibrite analüüsil selgus, et ühe tootja poolt valmistatud materjal ei sisaldanud, vastupidiselt tootja väidetele, boori, näidates välja töötatud meetodi vajalikkust.

Märksõnad: boor, basaltfiiber, MP-AES

CERCS: P300 analüütiline keemia